Am J Transl Res 2015;7(2):209-231
www.ajtr.org /ISSN:1943-8141/AJTR0002922

Original Article

Mixed serum-deprived and normal adipose-derived mesenchymal stem cells against acute lung ischemia-reperfusion injury in rats

Cheuk-Kwan Sun[1*], Steve Leu[2*], Shu-Yuan Hsu[3], Yen-Yi Zhen[4], Li-Teh Chang[5], Ching-Yen Tsai[6], Yung-Lung Chen[4], Yen-Ta Chen[7], Tzu-Hsien Tsai[4], Fan-Yen Lee[8], Jiunn-Jye Sheu[8], Hsueh-Wen Chang[9], Hon-Kan Yip[2,4,10]

[1]Department of Emergency Medicine, E-Da Hospital, I-Shou University, Kaohsiung, Taiwan; [2]Center for Translational Research in Biomedical Sciences, Kaohsiung Chang Gung Memorial Hospital and Chang Gung University College of Medicine, Kaohsiung, Taiwan; [3]Department of Anatomy, Graduate Institute of Biomedical Sciences, Chang Gung University Medical College, Taoyuan, Taiwan; [4]Division of Cardiology, Department of Internal Medicine, Kaohsiung Chang Gung Memorial Hospital and Chang Gung University College of Medicine, Kaohsiung, Taiwan; [5]Basic Science, Department of Nursing, Meiho University, Pingtung, Taiwan; [6]Institute of Molecular Biology, Academia Sinica, Taipei, Taiwan; [7]Division of Urology, Kaohsiung Chang Gung Memorial Hospital and Chang Gung University College of Medicine, Kaohsiung, Taiwan; [8]Division of Cardiovascular Surgery, Department of Surgery, Kaohsiung Chang Gung Memorial Hospital and Chang Gung University College of Medicine, Kaohsiung, Taiwan; [9]Department of Biological Sciences, National Sun Yat-Sen University, Kaohsiung, Taiwan; [10]Institute of Shock Wave Medicine and Tissue Engineering, Kaohsiung Chang Gung Memorial Hospital and Chang Gung University College of Medicine, Kaohsiung, Taiwan. [*]Equal contributors.

Received October 2, 2014; Accepted January 5, 2015; Epub February 15, 2015; Published February 28, 2015

Abstract: Background: This study hypothesized that combined serum-deprived (Sd) and healthy (He) adipose-derived mesenchymal stem cell (ADMSC) therapy is superior to either alone in reducing acute lung ischemia-reperfusion injury (ALIRI). Methods: Adult male Sprague-Dawley (SD) rats (n = 30) were equally randomized into group 1 (sham control), group 2 (ALIRI + culture medium), group 3 (ALIRI + intravenous autologous 1.2×10^6 He-ADMSCs at 30 minute, 6 h, and 24 h following lung ischemia/reperfusion for 45 minutes/72 hours, respectively), group 4 (ALIRI + 1.2×10^6 Sd-ADMSCs at identical time points after ischemia/reperfusion), and group 5 (ALIRI + 1.2×10^6 combined Sd-ADMSC/He-ADMSC 1:1). Results: Blood oxygen saturation (%) was lowest in group 2, lower in groups 3 to 5 than in group 1, and lower in group 5 than in group 1, whereas right ventricular systolic pressure (RVSP) showed a reverse pattern among the five groups (all $p < 0.001$). Additionally, changes in histological scoring of lung parenchymal damage, inflammatory and apoptotic biomarkers showed identical pattern compared to that of RVSP in all groups (all $p < 0.001$). Protein expressions of VCAM-1, ICAM-1, oxidative stress, TNF-α, nuclear factor-κB, and number of CD68 + cells were highest in group 2, higher in groups 3 to 5 than in group 1, and higher in groups 3 and 4 than in group 5, whereas NQO-1 and HO-1 activities and number of CD31 + and vWF + cells showed opposite changes compared with those of inflammatory biomarkers (all $p < 0.001$). Conclusion: Combined Sd-ADMSC/He-ADMSC therapy offered superior benefit to either option alone in minimizing rodent ALIRI through suppressing oxidative stress and inflammatory reaction.

Keywords: Lung ischemia-reperfusion injury, serum-deprived mesenchymal stem cell, cytotherapy, inflammation, oxidative stress

Introduction

Acute lung injury from diverse etiologies can result in remarkable in-hospital morbidity and mortality [1-3]. Previous studies have shed some light on several potential therapeutic strategies including the use of aprotinin [4], N-acetyl-L-cysteine [5], hypothermia [6], inhalational nitric oxide [7], and extracorporeal membrane oxygenator support [8]. However, the effectiveness of these treatment modalities is still controversial. Therefore, a safe and effective therapeutic regimen for patients with acute lung injury is still eagerly awaited.

Table 1. Flow cytometric analysis of He-ADMSC and Sd-ADMSC surface markers following Day 14 cell culture

Stem cell surface markers	He-ADMSC	Sd-ADMSC	*p*-value
CD31+	2.7 ± 0.6	3.8 ± 1.1	0.163
CD34+	11.3 ± 8.1	10.4 ± 4.3	0.409
VEGF+	26.1 ± 7.9	17.7 ± 3.1	0.025
CD133+	5.9 ± 4.8	3.6 ± 1.3	0.154
CD45+	13.4 ± 5.7	6.7 ± 4.0	0.022
C-kit+	15.8 ± 4.9	8.1 ± 3.2	0.024
Sca-1+	1.9 ± 0.7	1.8 ± 0.9	0.444
CD29+	98.9 ± 1.6	97.8 ± 4.2	0.290
CD90+	96.9 ± 2.9	89.8 ± 2.3	0.021
CD271+	24.5 ± 8.2	16.1 ± 3.2	0.029

Data are expressed as %. n = 6 in each experimental study. He = healthy (Refers to cells cultivated in normal medium); Sd = serum-deprived; ADMSC = adipose-derived mesenchymal stem cell; VEGF = vascular endothelial growth factor.

Previous histopathological and cellular-molecular studies have identified the roles of inflammatory cells, alveolar macrophages, and chemokines in mediating ischemia-reperfusion (IR) injury-elicited inflammation and oxidative stress in the lungs [8-11]. Pro-inflammatory cytokines and adhesion molecules that are upregulated following cellular activation have been shown to be crucial mediators in acute lung IR injury (ALIRI) [8-14]. Furthermore, local and systemic release of reactive oxygen species (ROS) also contributes to the destruction of pulmonary parenchyma, thereby causing a loss of alveolar capillary membrane integrity and an impairment of surfactant function [15, 16]. The latter is considered a hallmark of lung injury, leading to alveolar collapse and inadequate gaseous exchange [17].

Numerous clinical observational and experimental studies have established the safety and effectiveness of stem cell therapy in improving ischemia-related organ dysfunction [18-20]. Thus, stem cell therapy appears to be an attractive and promising treatment modality for cerebrovascular, cardiovascular, and peripheral vascular diseases refractory to conventional therapeutic options [18-23]. Surprisingly, in contrast to the abundance of studies [18-23] reporting the effectiveness of stem cell therapy for cerebral, cardiac, and vascular diseases, data addressing the effectiveness of stem cell treatment for acute lung injury are still limited [24, 25].

The mechanisms underlying the improvement of ischemia-related organ dysfunction following stem cell treatment have been demonstrated to involve the enhancement of angiogenesis, suppression of pro-inflammatory cytokine, promotion of stem cell homing, and contribution from paracrine effects [18, 19, 26, 27]. Moreover, some investigators have recently proposed that stem cell treatment can modulate immune reactivity through down-regulating innate and adaptive immunity [28]. One particularly intriguing finding is that apoptotic stem cells have been reported to possess a unique property of anti-inflammation and immune modulation [29]. Recently, we have shown that treatment with adipose-derived mesenchymal stem cells (ADMSCs) significantly minimized rodent ALIRI through suppressing oxidative stress and inflammatory reaction [30]. Since the mechanisms involved in ALIRI are complicated including the generation of ROS and a cascade of inflammatory processes [1-7], this study tested the hypothesis that treatment with apoptotic ADMSC through serum deprivation (Sd) may offer an additional benefit compared to healthy (He) ADMSC therapy alone in minimizing rat ALIRI through immunomodulation and suppression of oxidative stress and inflammatory reaction.

Methods

Ethics

All animal experimental procedures were approved by the Institute of Animal Care and Use Committee at Chang Gung Memorial Hospital-Kaohsiung Medical Center (Affidavit of Approval of Animal Use Protocol No. 2008121108) and performed in accordance with the Guide for the Care and Use of Laboratory Animals (NIH publication No. 85-23, National Academy Press, Washington, DC, USA, revised 1996).

Animal grouping, isolation of adipose tissue for culture of adipose-derived mesenchymal stem cells, and definition of He-ADMSCs and Sd-ADMSCs

Pathogen-free, adult male Sprague-Dawley (SD) rats (n = 30) weighing 350-400 g (Charles River Technology, BioLASCO Taiwan Co., Ltd., Taiwan) were randomized into group 1 (sham control, n = 6), group 2 (ALIRI plus culture medium, n = 6), group 3 [ALIRI + penile venous transfusion of autologous He-ADMSCs (1.2 ×

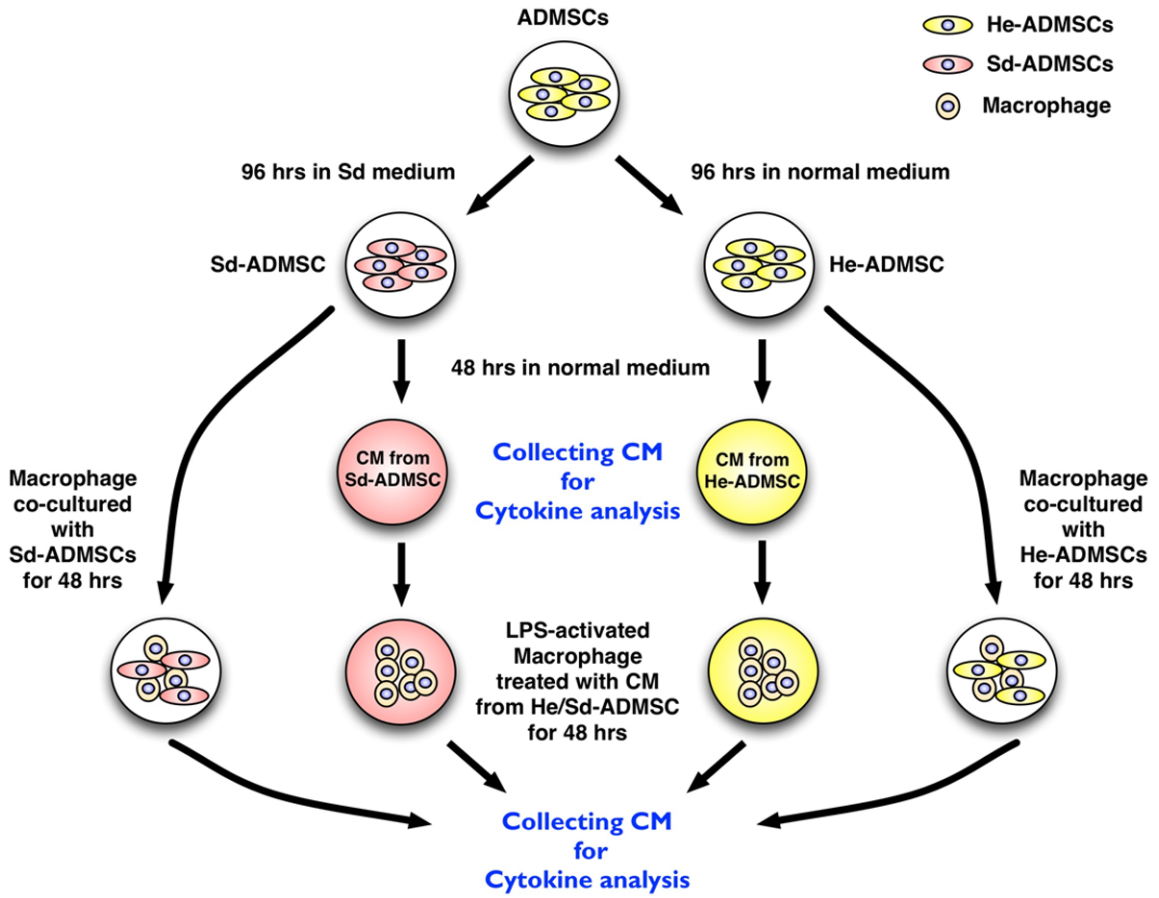

Figure 1. Experimental procedure and protocol. Procedures for 1) obtaining serum-deprived adipose-derived mesenchymal stem cells (Sd-ADMSCs), healthy adipose-derived mesenchymal stem cells (He-ADMSCs), and conditioned medium (CM, defined as medium from 48-hour ADMSC culturing) for co-culturing with macrophages; 2) for collection of conditioned media for ELISA analyses of anti-inflammatory cytokines; and 3) for collection of conditioned media from co-culturing macrophages under different conditions for ELISA analyses of anti-inflammatory cytokines. *indicated co-culturing macrophages with conditioned medium and fresh culture medium (1:1 by volume).

10^6) at 30 minute, 6 h, and 24 h after the procedure, n = 6)], group 4 [ALIRI + autologous Sd-ADMSCs (1.2×10^6) at 30 minute, 6 h, and 24 h after the procedure, n = 6] and group 5 (ALIRI + 1.2×10^6 combined He-ADMSCs and Sd-ADMSCs, 1:1, at identical time points, n = 6).

The rats in groups 3, 4, and 5 were anesthetized with inhalational isoflurane 14 days before induction of ALIRI. Adipose tissue surrounding the epididymis was carefully dissected, excised, and prepared based on our recent report [30]. Briefly, adipose tissue surrounding the epididymis was carefully dissected and excised. The isolated ADMSCs were cultured in a 100 mm diameter dish with 10 mL DMEM culture medium containing 10% FBS for 7 days. Flow cytometric analysis was performed for identification of cellular characteristics after cell-labeling with appropriate antibodies on day 14 of cell cultivation prior to implantation (**Table 1**).

He-ADMSCs were those cultured in normal culture medium with adequate nutritional supply. On the other hand, since serum deprivation of cells in vitro has been documented to induce apoptosis [31]. Sd-ADMSCs were first cultured in normal culture medium followed by 48 hours of serum deprivation after which the expressions of apoptotic proteins were determined by Western blot and immunofluorescent staining. In addition, the percentages of viable and dead cells were also determined by flow cytometric analysis using double staining of annexin V and propidium iodide (PI) which is a simple and popular method for the identification of apoptotic cells [i.e. early phase of (annexin V +/PI-) and late phase (annexin V +/PI +) of apoptosis].

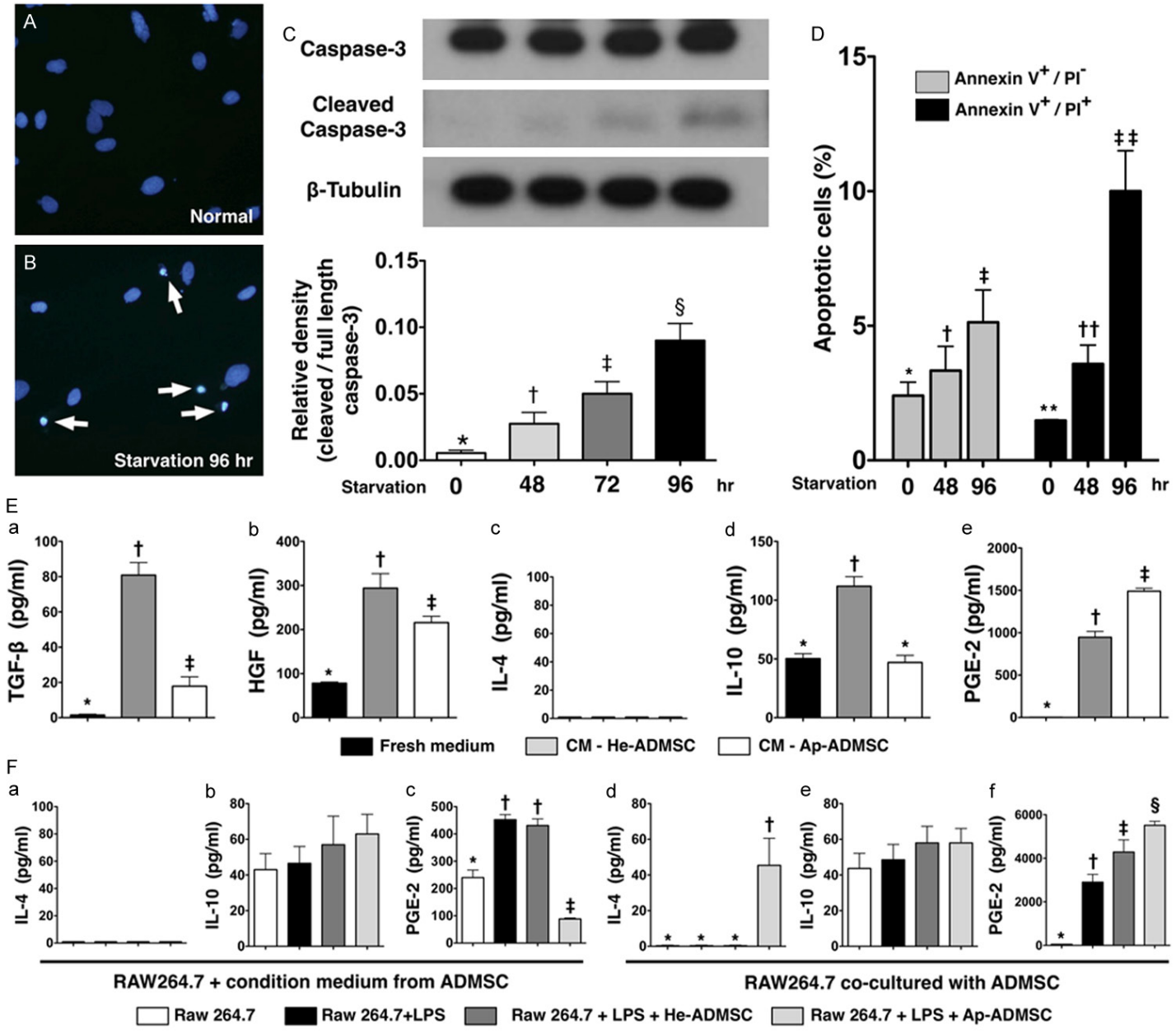
A
Normal
B
Starvation 96 hr
C
Caspase-3
Cleaved Caspase-3
β-Tubulin
Relative density (cleaved / full length caspase-3)
Starvation 0 48 72 96 hr
D
Annexin V+ / PI-
Annexin V+ / PI+
Apoptotic cells (%)
Starvation 0 48 96 0 48 96 hr
E
a TGF-β (pg/ml)
b HGF (pg/ml)
c IL-4 (pg/ml)
d IL-10 (pg/ml)
e PGE-2 (pg/ml)
Fresh medium
CM - He-ADMSC
CM - Ap-ADMSC
F
a IL-4 (pg/ml)
b IL-10 (pg/ml)
c PGE-2 (pg/ml)
d IL-4 (pg/ml)
e IL-10 (pg/ml)
f PGE-2 (pg/ml)
RAW264.7 + condition medium from ADMSC
RAW264.7 co-cultured with ADMSC
Raw 264.7
Raw 264.7+LPS
Raw 264.7 + LPS + He-ADMSC
Raw 264.7 + LPS + Ap-ADMSC

Figure 2. Results of in vitro studies (western blotting, immunofluorescent staining, and ELISA). A and B. Immunofluorescent staining showing condensed apoptotic nuclei (white arrows) of adipose-derived mesenchymal stem cells (Sd-ADMSCs) in serum-deprived culture medium for 96 hours and blue oval normal nuclei after counterstaining with DAPI. C. Western blotting showing significant stepwise elevation in cleaved caspase-3 protein expression after different durations of serum deprivation. *vs. other bars with different symbols, $p < 0.0001$. D. Flow cytometric analysis demonstrating significant increase in cellular apoptosis in both early (annexin V +/PI-) and late (annexin V +/PI +) phases at respective time points of starvation. PI = propidium iodide stain. *vs. other bars with different symbols, $p < 0.001$. **vs. other bars with different symbols, $p < 0.0001$. E. ELISA of fresh culture medium and conditioned medium (CM) from either healthy adipose-derived mesenchymal stem cells (He-ADMSCs) (i.e., those cultured in normal medium) or Sd-ADMSCs showing levels of (a) transforming growth factor-β (TGF-β), (b) hepatocyte growth factor (HGF), (c) interleukin (IL)-4, (d) IL-10, and (e) prostaglandin E (PGE)-2. *vs. other bars with different symbols, $p < 0.0001$. F. Concentration of cytokines in conditioned media from co-culturing macrophages under different conditions. (a & d) IL-4, (b & e) IL-10, and (c & f) PGE-2. *vs. other bars with different symbols, $p < 0.0001$. All statistical analyses using one-way ANOVA, followed by Bonferroni multiple comparison post hoc test. Symbols (*, †, ‡, § or **, ††, ‡‡) indicate significance (at 0.05 level). LPS = lipopolysaccharide.

The procedure and protocol of in vitro studies for determining anti-inflammatory/immunomodulatory effects of He-ADMSCs and Sd-ADMSCs

To compare the anti-inflammatory and immunomodulatory properties between He-ADMSCs and Sd-ADMSCs, cell culture (n = 6 for each study) was performed in He-ADMSCs and Sd-ADMSCs (with initial starvation for 96 h, follow by culturing in normal culture medium) for 48 h (**Figure 1**). The medium was collected after 48 h cell culture for ELISA to determine the levels of interleukin (IL)-10, IL-4, prostaglandin E (PGE)-2, hepatocyte growth factor (HGF), and transforming growth factor (TGF)-β, indices of anti-inflammation/immunomodulation.

Furthermore, to determine whether the cellular elements (i.e. He-ADMSCs and Sd-ADMSCs) or conditioned medium (i.e., culture medium from cultivation of He- or Sd-ADMSCs + fresh medium, 1:1 by volume) could transform the property of macrophages from immunoreactive to immunomodulatory, the mouse leukemic monocyte macrophage cell line (1.0×10^5) (RAW 264.7 purchased from ATCC) was co-cultured with He-ADMSCs (1.0×10^5), Sd-ADMSCs (1.0×10^5), and both conditioned media for 48 hours in the presence of lipopolysaccharide (LPS 1 μg/mL) for 3 hours. The culture media were then collected for determining the levels of IL-4, IL-10, and prostaglandin E (PGE)-2 using ELISA.

CM-DiI labelling of both He-ADMSCs and Sd-ADMSCs, protocol of experiment, and autologous ADMSC transfusion

The detailed protocol and procedure of lung IR was as described in our recent study [30]. Briefly, all animals were anesthetized by 2.0% inhalational isoflurane and placed in a supine position on a warming pad at 37°C, followed by endotracheal intubation with positive-pressure ventilation (180 mL/min) with room air using a Small Animal Ventilator (SAR-830/A, CWE, Inc., USA). Under sterile conditions, lung IR was conducted in groups 2, 3, 4, and 5 animals on which a left thoracotomy was performed and the left proximal pulmonary artery and main bronchus were totally clamped for 45 minutes using non-traumatic vascular clips before reperfusion for 72 h. Sham-operated rats subjected to left thoracotomy only served as normal controls.

CM-DiI (Vybrant™ DiI cell-labeling solution, Molecular Probes, Inc.) (50 μg/mL) was added to the culture medium 30 minutes before the IR procedure for He-ADMSC and Sd-ADMSC labeling. After completion of ADMSC labeling, intravenous injection of autologous He-ADMSCs (1.2×10^6), Sd-ADMSCs (1.2×10^6), and combined mixed He- and Sd-ADMSCs (1:1) for the respective group was performed through the penile vein 30 minutes after the procedure, followed by intravenous infusion at 6 h and 24 h following IR of the lungs. The dosage of ADMSCs utilized in the current study was based on our recent report [30]. At 72 h after the IR procedure, left thoracotomy was performed for all animals. The presence of pleural effusion was noted and the right ventricular systolic blood pressure (RVSBP), an indicator of pulmonary arterial blood pressure, was measured for all animals immediately before sacrificing the animals. The left lungs were collected for individual study.

For tracking the injected ADMSCs, the *In Vivo* Imaging Systems (IVIS spectrum, Xenogen) was

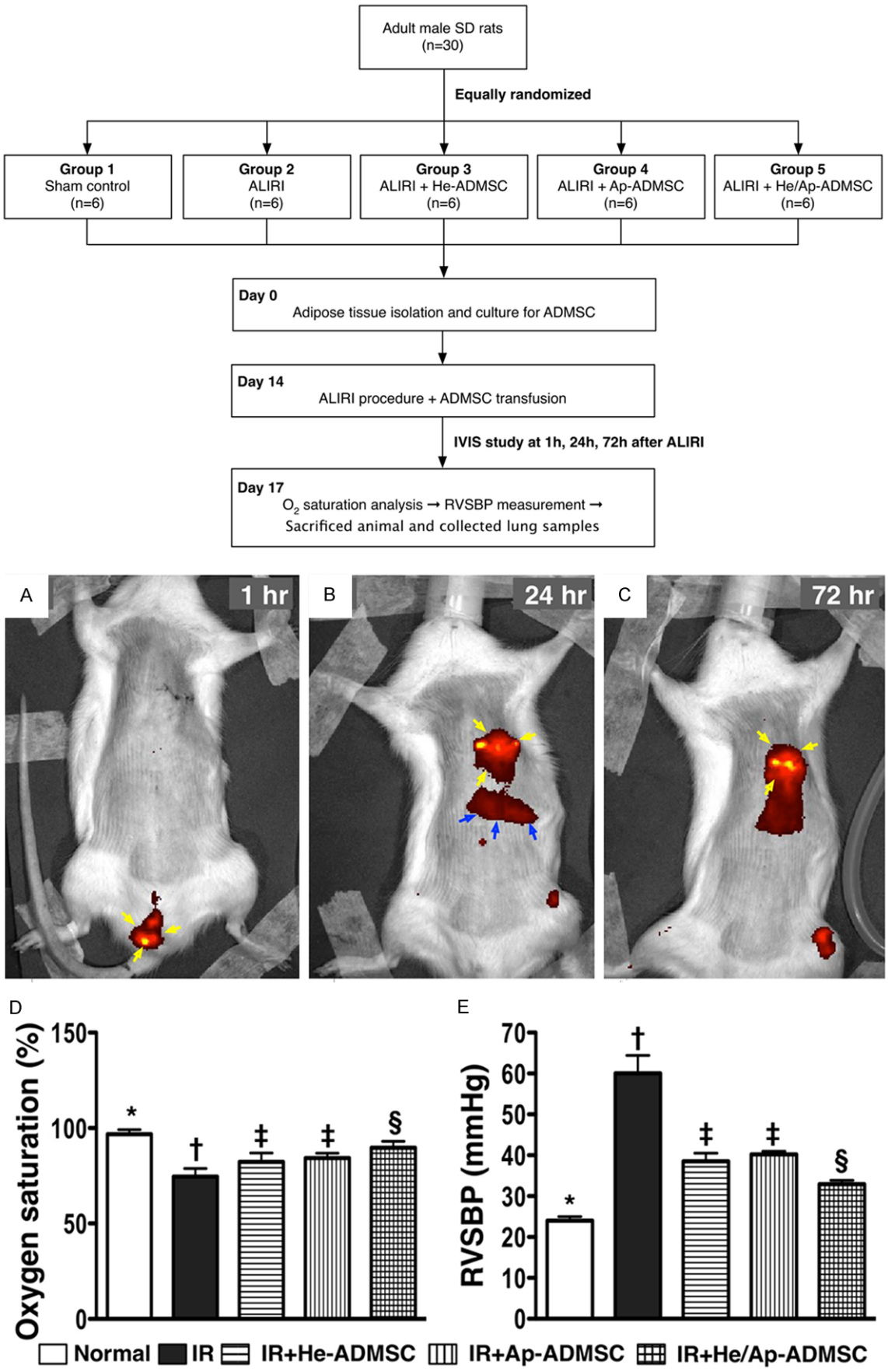
Adult male SD rats
(n=30)
Equally randomized
Group 1
Sham control
(n=6)
Group 2
ALIRI
(n=6)
Group 3
ALIRI + He-ADMSC
(n=6)
Group 4
ALIRI + Ap-ADMSC
(n=6)
Group 5
ALIRI + He/Ap-ADMSC
(n=6)
Day 0
Adipose tissue isolation and culture for ADMSC
Day 14
ALIRI procedure + ADMSC transfusion
IVIS study at 1h, 24h, 72h after ALIRI
Day 17
O_2 saturation analysis → RVSBP measurement →
Sacrificed animal and collected lung samples
A
1 hr
B
24 hr
C
72 hr
D
Oxygen saturation (%)
150
100
50
0
E
RVSBP (mmHg)
70
60
50
40
30
20
10
0
Normal
IR
IR+He-ADMSC
IR+Ap-ADMSC
IR+He/Ap-ADMSC

Figure 3. Tracking infused stem cells using In Vivo Imaging System (IVIS) and comparison of arterial oxygen saturation and right ventricular systolic blood pressure (RVSBP) at 72 h after lung ischemia reperfusion (IR). A. Red patches (yellow arrows) around penile region indicating DiR-labelled (specific IVIS dye) adipose-derived mesenchymal stem cells (ADMSCs). B. Distribution of DiR-labelled ADMSCs around left lung field (yellow arrows) and liver (blue arrows) by post-IR 24 h. C. Persistent presence of ADMSCs (yellow arrows) over left lung field at 72 h after IR procedure. D. Arterial oxygen saturation (%) at post-IR 72 h. *vs. other bars with different symbols, $p < 0.001$. E. Right ventricular systolic blood pressure (RVSBP) at post-IR 72 h prior to sacrificing the animals. *vs. other bars with different symbols, $p < 0.0001$. All statistical analyses using one-way ANOVA, followed by Bonferroni multiple comparison post hoc test. Symbols (*, †, ‡, §) indicating significance (at 0.05 level). He-ADMSC = healthy ADMSC (i.e. cultivated in normal medium); Sd-ADMSC = serum-deprived ADMSC. (n = 6 in each group).

utilized at 1 h, 24 h, and 72 h after the lung IR procedure with the ADMSCs being pre-labeled with a specific IVIS dye (i.e. DiR) (**Figure 3**) in 2 additional rats.

Determination of oxygen saturation (%) and right ventricular systolic blood pressure (RVSBP)

To examine the effect of ADMSC treatment on arterial oxygen saturation (% of Sat O_2), arterial blood was sampled from the tail artery for blood gas analysis prior to left thoracotomy and at 72 h after the IR procedure prior to intubation and ventilator use. For RVSBP measurement, each animal was endotracheally intubated with positive-pressure ventilation (180 mL/min) with room air using a small animal ventilator. The detailed procedure was described in our recent report [30]. After hemodynamic measurements, the rats were euthanized with the hearts and lungs harvested and weighted. Half of left lung was fixed in 4% formaldehyde and then embedded in paraffin blocks. The remaining left lung was cut into pieces, frozen in liquid nitrogen and then stored at -80°C until later use.

Histological assessment of lung injury and crowded score of lung parenchyma

For identification of alveolar sac distribution in lung parenchyma, left lung specimens from all animals were fixed in 10% buffered formalin before embedding in paraffin and the tissue was sectioned at 5 μm for light microscopic analysis. Hematoxylin and eosin (H & E) staining was performed to determine the number of alveolar sacs according to our recent study [30] in a blind fashion. Three lung sections from each rat were analyzed and three randomly selected high-power fields (HPFs) (100 ×) were examined in each section. The mean number per HPF for each animal was then determined by summation of all numbers divided by 9. In addition, alveolar wall thickness and the presence or absence of hemorrhage were determined under light microscopy. The extent of crowded area, which was defined as region of thickened septa in lung parenchyma associated with partial or complete collapse of alveoli on H & E-stained sections, was performed in a blind fashion. The scoring system adopted was as follows: 0 = no detectable crowded area; 1 = < 15% of crowded area; 2 = 15-25% of crowded area; 3 = 25-50% of crowded area; 4 = 50-75% of crowded area; 5 = > 75%-100% of crowded area/per high-power filed (100 ×).

Immunohistochemical (IHC) and immunofluorescent (IF) studies

The procedure and protocol of IHC and IF examinations were also based on our recent study [30]. For IHC staining, rehydrated paraffin sections were first treated with 3% H_2O_2 for 30 minutes and incubated with Immuno-Block reagent (BioSB) for 30 minutes at room temperature. Sections were then incubated with primary antibodies specifically against glutathione peroxidase (GP ×) (1:500, Abcam) and glutathione reductase (GR) (1:100, Abcam) at 4°C overnight. Irrelevant antibodies [(p53, 1:500 (Abcam) and mouse control IgG (Abcam)] were used as controls in the current study. IF staining was performed for the examinations of CD68 (macrophage surface marker) (1:100 Abcam), CD31 (1:200, SeroTec), and von Willebrand factor (vWF) (1:200, Millipore) using respective primary antibodies. Irrelevant antibodies were used as controls in the current study. Three sections of lung specimens were analyzed in each rat. For quantification, three randomly selected HPFs (× 200 for IHC and IF stain respectively) were analyzed in each section. The mean number per HPF for each animal was then determined by summation of all numbers divided by 9.

An IHC-based scoring system was adopted for semi-quantitative analyses of GR and GPx as percentage of positive cells in a blind fashion [Score of positively-stained cell for GR and GPx:

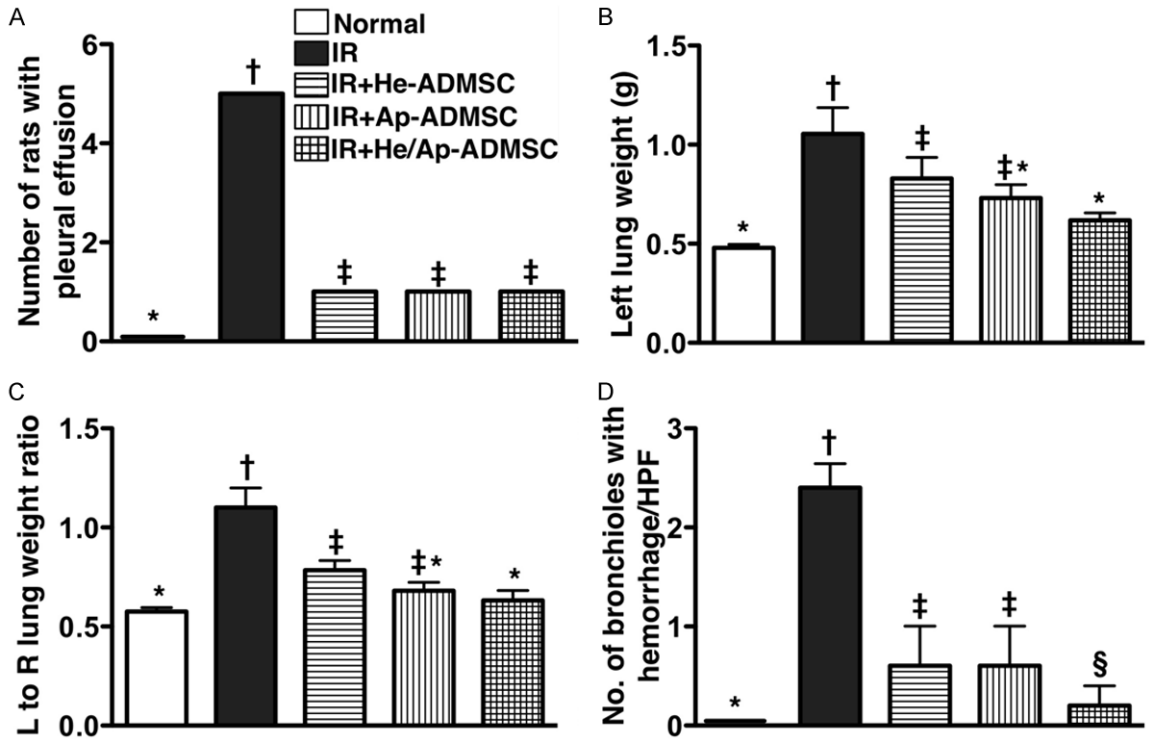

Figure 4. Gross pulmonary pathological changes at 72 h after ischemia-reperfusion (IR). A. The number of rats with bloody pleural effusion in each group. *vs. other bars with different symbols, $p < 0.0001$. *vs. other bars with different symbols, $p < 0.001$. B. Comparison of left lung weight among the five animal groups at post-IR 72 h. *vs. other bars with different symbols, $p < 0.001$. C. The ratio of left (L) to right (R) lung weight. *vs. other bars with different symbols, $p < 0.0001$. D. Comparison of the number of bronchioles with hemorrhage per high-power field (HPF) (100x) among the five groups (P.S. Please refer to hematoxylin eosin-stained sections in **Figure 4**). *vs. other bars with different symbols, $p < 0.0001$. All statistical analyses using one-way ANOVA, followed by Bonferroni multiple comparison post hoc test. Symbols (*, †, ‡, §) indicating significance (at 0.05 level). He-ADMSC = healthy ADMSC (i.e. cultivated in normal medium); Sd-ADMSC = serum-deprived ADMSC. (n = 6 in each group).

0 = no stain %; 1 = < 15%; 2 = 15~25%; 3 = 25~50%; 4 = 50~75%; 5 = > 75%-100%/per high-power filed (200 ×)].

Western blot analysis of left lung specimens

Equal amounts (10-30 μg) of protein extracts from the left lung were loaded and separated by SDS-PAGE using 8-10% acrylamide gradients. Following electrophoresis, the separated proteins were transferred electrophoretically to a polyvinylidene difluoride (PVDF) membrane (Amersham Biosciences). Nonspecific proteins were blocked by incubating the membrane in blocking buffer (5% nonfat dry milk in T-TBS containing 0.05% Tween 20) overnight. The membranes were incubated with monoclonal antibodies against vascular cell adhesion molecule (VCAM)-1 (1:100, Abcam), intercellular adhesion molecule (ICAM)-1 (1:2000, Abcam), NAD(P)H quinone oxidoreductase (NQO)-1 (1:1000, Abcam), heme oxygense (HO)-1 (1:250, Abcam), and polyclonal antibodies against TNF-α (1:1000, Cell Signaling), NF-κB (1:250, Abcam), Bax (1:1000, Abcam), caspase 3 (1:1000, Cell Signaling), poly(ADP-ribose) polymerase (PARP) (1:1000, Cell Signaling), and Bcl-2 (1:250, Abcam). Signals were detected with horseradish peroxidase (HRP)-conjugated goat anti-mouse, goat anti-rat, or goat anti-rabbit IgG.

The Oxyblot Oxidized Protein Detection Kit was purchased from Chemicon (S7150). The procedure of 2,4-dinitrophenylhydrazine (DNPH) derivatization was carried out on 6 μg of protein for 15 minutes according to manufacturer's instructions. One-dimensional electrophoresis was carried out on 12% SDS/polyacrylamide gel after DNPH derivatization. Proteins were transferred to nitrocellulose membranes which were then incubated in the primary antibody

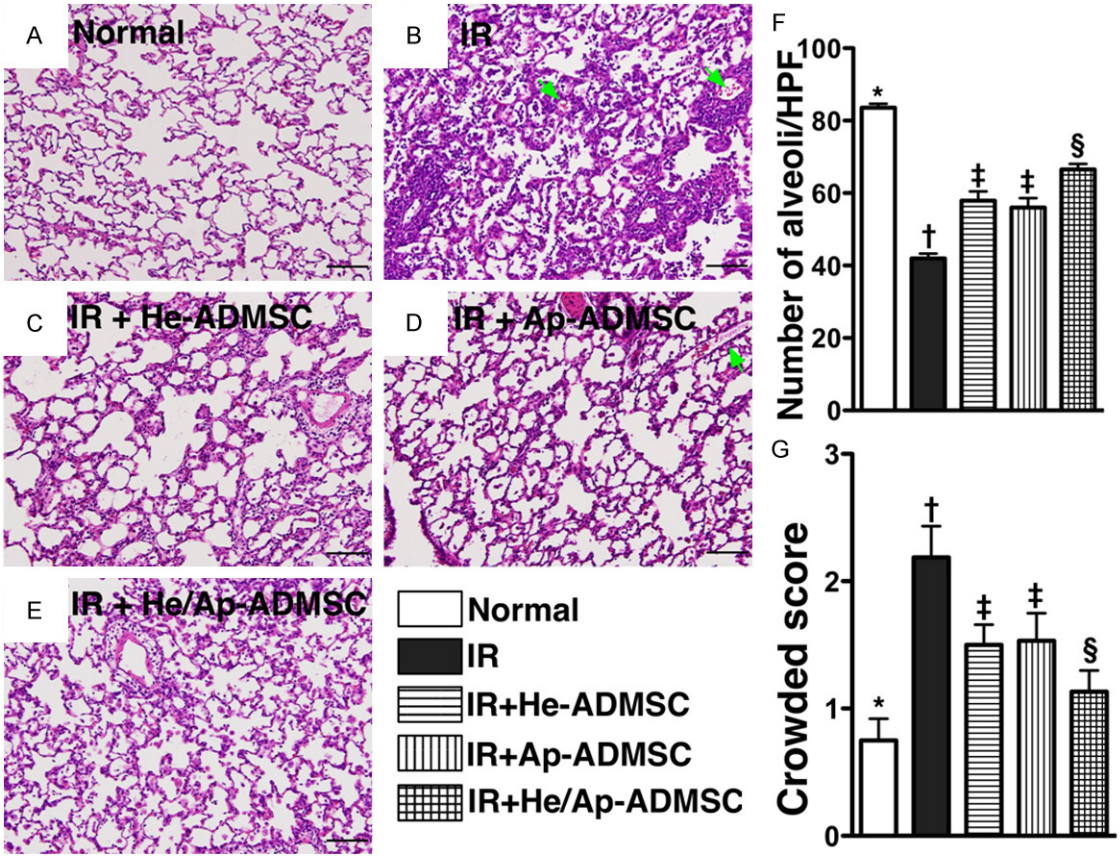

Figure 5. Pathological findings of left lung parenchyma (100x) at 72 h after ischemia-reperfusion (IR). A to E. Hematoxylin and eosin staining of left lung parenchyma at post-IR 72 h. Green arrows indicating hemorrhage in bronchioles. F. The number of intact alveoli per high-power field (100x) among the five groups. *vs. other bars with different symbols, $p < 0.0001$. G. The crowded score of left lung at 72 h after lung IR. *vs. other bars with different symbols, $p < 0.001$. Scale bars in right lower corner represent 100 μm. All statistical analyses using one-way ANOVA, followed by Bonferroni multiple comparison post hoc test. Symbols (*, †, ‡, §, ¶) indicating significance (at 0.05 level). He-ADMSC = healthy ADMSC (i.e. cultivated in normal medium); Sd-ADMSC = serum-deprived ADMSC. (n = 6 in each group).

solution (anti-DNP 1:150) for two hours, followed by incubation with secondary antibody solution (1:300) for one hour at room temperature. The washing procedure was repeated eight times within 40 minutes.

Immunoreactive bands were visualized by enhanced chemiluminescence (ECL; Amersham Biosciences) which was then exposed to Biomax L film (Kodak). For quantification, ECL signals were digitized using Labwork software (UVP). For oxyblot protein analysis, a standard control was loaded on each gel.

Real-Time quantitative PCR analysis

The mRNA expressions of matrix metalloproteinase (MMP)-9, tumor necrosis factor (TNF)-α, nuclear factor kappa-light-chain-enhancer of activated B cells (NF-κB), heme oxygense (HO)-1, NAD(P)H quinone oxidoreductase (NQO) 1, glutathione reductase (GR), and glutathione peroxidase (GPx), IL-10, IL-12, endothelial nitric oxide synthase (eNOS), and endothelin-1 (ET-1) of the five groups of animals were analyzed with RT-qPCR and compared. Technical details were according to those previously described [30].

Statistical analysis

Quantitative data are expressed as means ± SD. Statistical analysis was adequately performed by ANOVA followed by Bonferroni multiple-comparison post hoc test. Statistical analysis was performed using SAS statistical software for Windows version 8.2 (SAS institute, Cary, NC). A probability value < 0.05 was considered statistically significant.

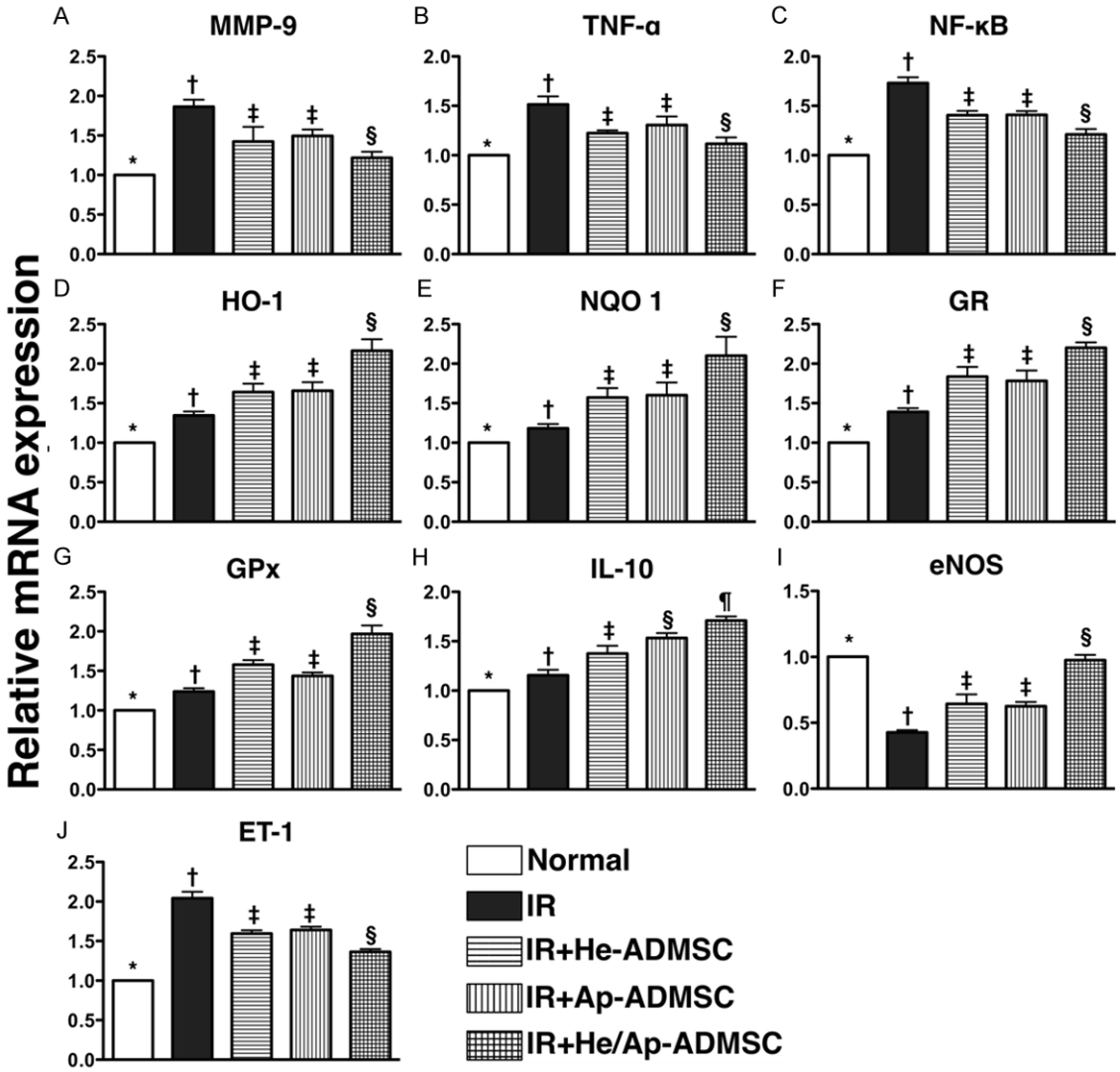

Figure 6. mRNA expressions of inflammatory, anti-oxidant, anti-inflammatory, and endothelial dysfunctional biomarkers in left lung at 72 h after ischemia-reperfusion. A-C. mRNA expressions of matrix metalloproteinase (MMP)-9, tumor necrotic factor (TNF)-α, and nuclear factor (NF)-κB. *vs. other bars with different symbols, $p < 0.0001$. D-G. mRNA expressions of heme oxygense (HO)-1, NAD(P)H quinone oxidoreductase (NQO) 1, glutathione reductase (GR) and glutathione peroxidase (GPx). *vs. other bar with different symbols, $p < 0.0001$. H. mRNA expression of interleukin (IL)-10. *vs. other bars with different symbols, $p < 0.001$. I. Endothelial nitric oxide synthase (eNOS) mRNA expression. *vs. other bars with different symbols, $p < 0.0001$. J. Endothelin (ET)-1 mRNA expression. *vs. other bars with different symbols, $p < 0.0001$. Symbols (*, †, ‡, §, ¶) indicating significance (at 0.05 level). IR = ischemia-reperfusion; He-ADMSC = healthy ADMSC (i.e. cultivated in normal medium); Sd-ADMSC = serum-deprived ADMSC. (n = 6 in each group).

Results

In vitro studies

As expected, immunofluorescent staining, Western blot, and flow cytometric analysis identified significantly more apoptotic ADMSCs after 96 hours of Sd culturing (**Figure 2A-D**) (i.e., Sd-ADMSCs). Additionally, the levels of TGF-β, HGF, IL-4, and IL-10 were significantly lower in the culture medium for Sd-ADMSCs compared to those for He-ADMSCs (**Figure 2Ea-Ee**), whereas the PGE-2 level showed a reversed pattern.

Surprisingly, IL-4 was not detected in the culture media from macrophage only (group A), macrophage + LPS (group B), and macrophage

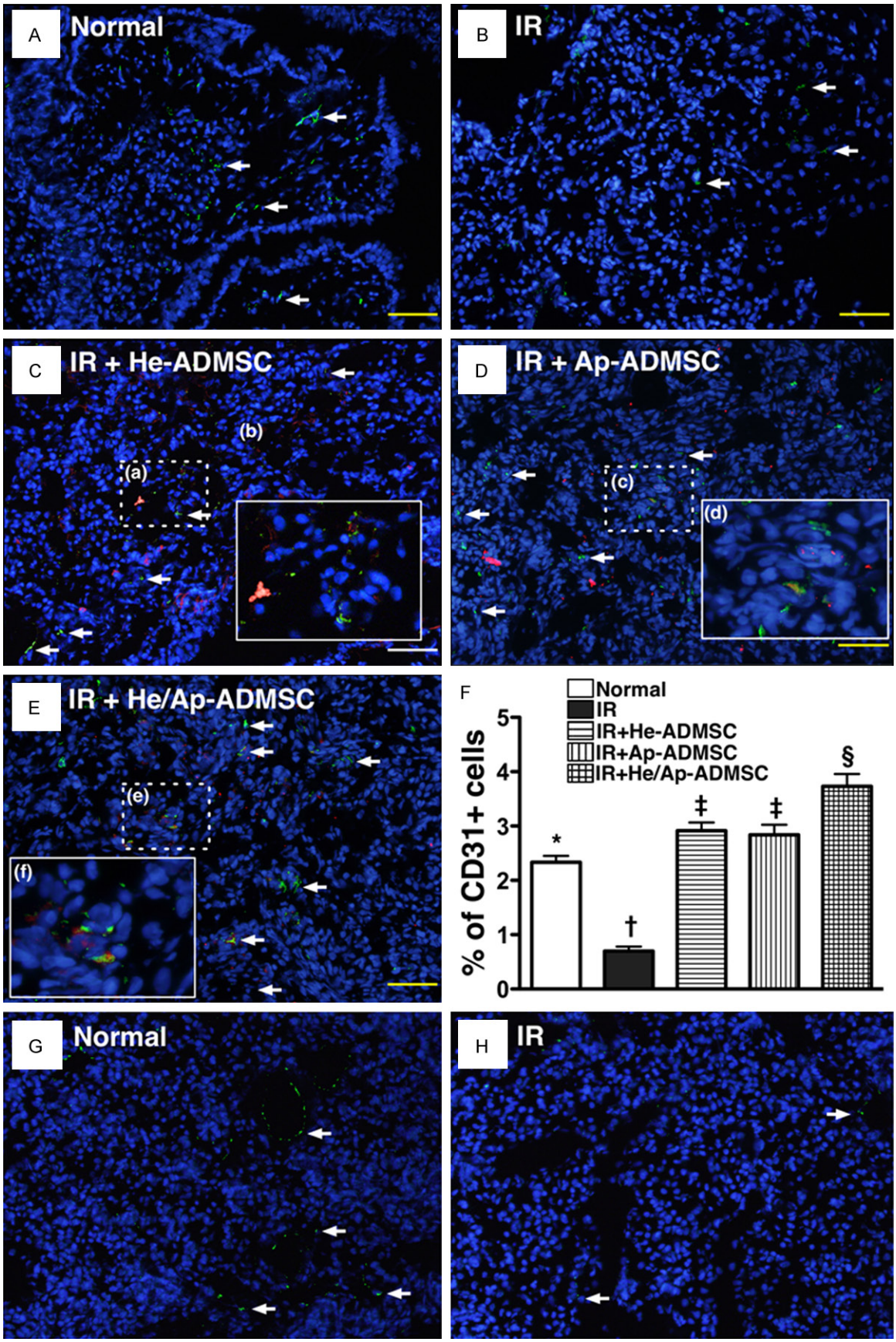
A
Normal
B
IR
C
IR + He-ADMSC
(a)
(b)
D
IR + Ap-ADMSC
(c)
(d)
E
IR + He/Ap-ADMSC
(e)
(f)
F
Normal
IR
IR+He-ADMSC
IR+Ap-ADMSC
IR+He/Ap-ADMSC
% of CD31+ cells
0
1
2
3
4
5
*
†
‡
‡
§
G
Normal
H
IR

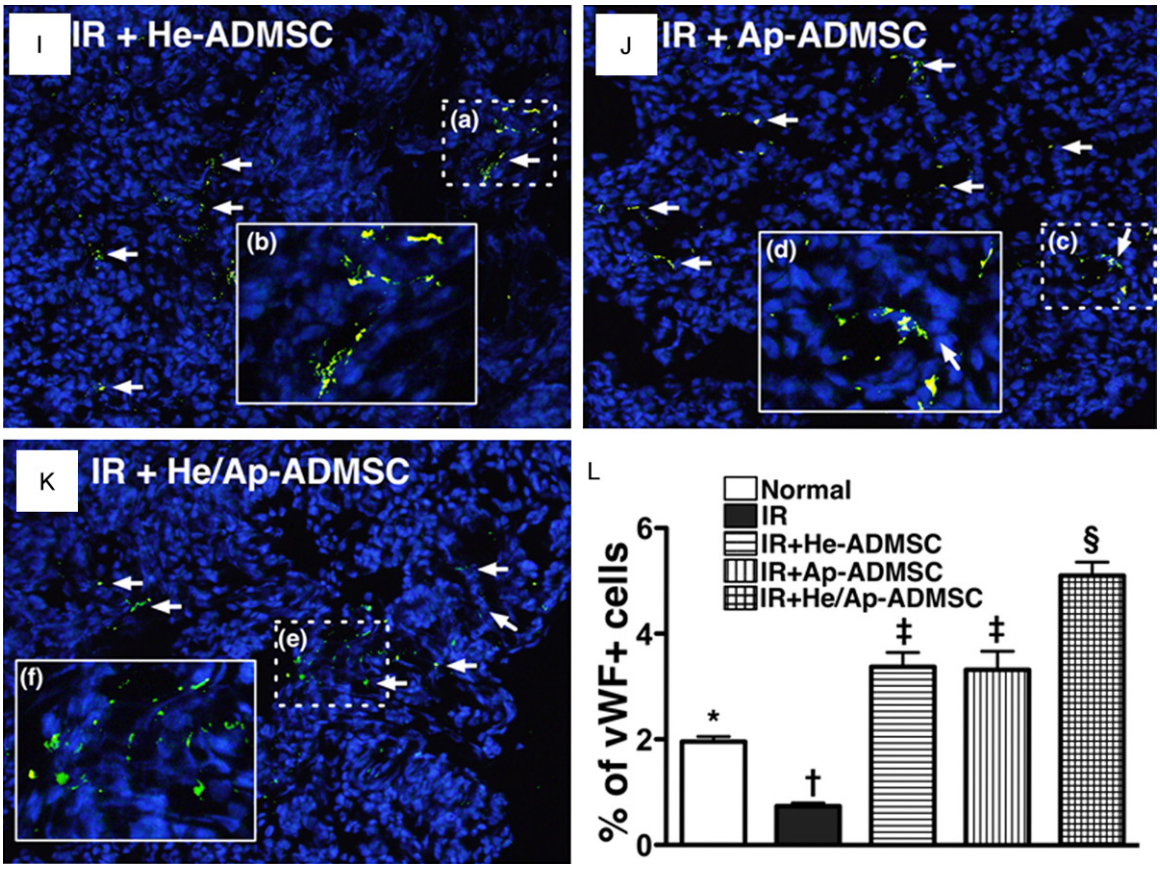

Figure 7. Prevalence of CD31+ and von Willebrand Factor (vWF)+ cells in left lung parenchyma at 72 h after ischemia-reperfusion (IR). (A-D) Immunofluorescent (IF) staining (200x) of CD31+ cells (green) in lung parenchyma. Notably fewer CD31+ cells (white arrows) in IR group (B) than in other groups (A, C-E). (C-E) Merged image from double staining (DiI + CD31) showing cellular elements of mixed red and yellow under high magnifications (400x) [(b), (d), and (f) being magnified images of (a), (b), and (c), respectively], indicating implanted CD31+ cells in lung parenchyma. (F) *vs. other bars with different symbols, $p < 0.0001$. G to K) IF staining (200x) showing von Willebrand factor (vWF)+ cells (green) in lung parenchyma. Notably reduced number of vWF+ cells (white arrows) in IR group (H) than in other groups (G, I-K). I-K. Merged image from double staining (DiI + vWF) demonstrating cellular elements with mixed red and yellow under high magnifications (400x) [(b), (d), and (f) being magnified images of (a), (b), and (c), respectively], indicating implanted vWF+ cells in lung parenchyma. (L) *vs. other bars with different symbols, $p < 0.0001$. *vs. other bars with different symbols, $p < 0.0001$. Symbols (*, †, ‡, §) indicating significance (at 0.05 level). He-ADMSC = healthy ADMSC (i.e. cultivated in normal medium); Sd-ADMSC = serum-deprived ADMSC. Scale bars in right lower corners represent 50 μm. (n = 6 in each group).

+ LPS + conditioned medium derived from either He-ADMSCs (group C) or Sd-ADMSCs (group D) (**Figure 2Fa**). Additionally, the IL-10 level in culture medium did not differ among these four groups (**Figure 2Fb**). However, the PGE-2 level was lowest in group D, lower in group A than in groups B and C, but it exhibited no difference between group B and C (**Figure 2Fc**).

Although the IL-4 level in culture media was too low to be detected in groups A, B, and E (i.e., macrophage + LPS + He-ADMSCs) (**Figure 2Fd**), its level was remarkably higher in group F (i.e., macrophage + LPS + Sd-ADMSCs) than in other groups (**Figure 2Fd**). On the other hand, the IL-10 level in culture media was similar among the four groups (**Figure 2Fe**). By contrast, the PGE-2 level was notably higher in group E than in other groups and significantly higher in group F than in groups A and B, while it displayed no difference between groups A and B (**Figure 2Ff**).

Flow cytometric analyses of adipose-derived stem cell surface markers at day 14 of cell cultivation

Surface markers of endothelial progenitor cell (EPCs) (CD31 +, CD34 +, CD133 +), endothelial

cell (VEGF +) and MSC (CD45 +, C-kit +, Sca-1 +, CD29 +, CD90 +, CD271 +) were examined for He-ADMSCs and Sd-ADMSCs using flow cytometry at day 14 of cell culturing (**Table 1**). The percentages of all EPC surface markers were similar between Sd-ADMSCs and He-ADMSCs. Additionally, the percentages of the MSC surface markers of Sca-1 + and CD29 + cells also did not differ between Sd-ADMSCs and He-ADMSCs (**Table 1**). However, the expression of endothelial cell surface marker of VEGF was significantly higher in He-ADMSCs than in Sd-ADMSCs. Furthermore, as compared with Sd-ADMSCs, the percentage of MSC surface marker of C-kit, CD90 + and CD271 + cells were significantly higher in He-ADMSCs after 14 days of cell cultivation (**Table 1**).

The use of IVIS for confirmation of ADMSC sequestration in lung parenchyma after transfusion

Interestingly, the IVIS demonstrated that the majority of transfused ADMSCs were found to be mainly located in the penile area 1 h after the procedure (**Figure 3A**). However, these cells were found to be mainly sequestrated in left lung area 24 h after the lung IR procedure (**Figure 3B**) and persistently present in the left lung 72 h after lung IR procedure (**Figure 3C**).

Arterial oxygen saturation and right ventricular systolic blood pressure 72 hours after lung IR

The percentage of arterial oxygen saturation (Sat O_2, %) did not differ among the normal controls (group 1), ALIRI rats (group 2), and ALIRI + He-ADMSCs treated rats (group 3), ALIRI + Sd-ADMSCs treated rats (group 4), and ALIRI + combined treatment with both ADMSCs (group 5) prior to the IR procedure (94.8%, 94.3%, 93.7%, 94.1%, and 95.0%, respectively, $p > 0.5$) (**Figure 3D**). However, Sat O_2 was significantly higher in group 1 than in groups 2 to 5, significantly higher in group 5 than in groups 2 to 4, and notably higher in groups 3 and 4 than in group 2, but it showed no difference between groups 3 and 4 at 72 h after the IR procedure (**Figure 3D**). Conversely, RVSBP showed opposite changes compared with that of Sat O_2 among the five groups (**Figure 3E**).

Gross anatomical and histopathological changes of left lung parenchyma

No right or left pleural effusion was present in group 1 (**Figure 4A**). In addition, no right pleural effusion was noted among groups 2 to 5. However, minimal left bloody pleural effusion (< 1.0 mL) was observed in one animal during thoracotomy from groups 3 to 5 (17% in each group). On the other hand, larger amount (> 1.0 mL) of left pleural effusion was present in 5 animals of group 2 (i.e. the untreated group) (83%). Hence, the incidence of bloody left pleural effusion was remarkably higher in group 2 than in other groups without remarkable difference among other IR groups.

The weight of left lung was substantially higher in group 2 than in other groups, significantly higher in groups 3 than in groups 1 and 5, but it exhibited no difference between groups 3 and 4 or among groups 1, 4, and 5 (**Figure 4B**). The ratio of left to right lung weight showed an identical pattern compared to that of left lung weight among the five groups (**Figure 4C**).

To evaluate the impact of ADMSC transplantation on the severity of IR-induced lung parenchymal injury, H & E-stained lung sections were examined (**Figure 5**). Intra-tracheal hemorrhage was more frequently observed in group 2, but it displayed no difference among the other IR groups (**Figures 4D** & **5**). Moreover, the number of alveolar sacs in left lung was substantially fewer in group 2 than in other groups, markedly reduced in groups 3 and 4 than in groups 1 and 5, notably lower in group 5 than in group 1, but was similar between groups 3 and 4 (**Figure 5E**). By contrast, the lung parenchyma was remarkably crowded in group 2 compared with that in other lung IR groups, notably more crowded in groups 3 and 4 than in groups 1 and 5, and was significantly more crowded in group 5 compared to that of group 1, but it showed no difference between groups 3 and 4 (**Figure 5G**). Furthermore, the frequency of alveolar septal thickening showed an identical pattern compared to that of lung parenchyma crowding among the five groups (**Figure 5**).

Autologous ADMSC transfusion limited mRNA expressions of markers of inflammation, oxidative stress, and endothelial dysfunction in lung parenchyma after IR injury

The mRNA expressions of MMP-9, TNF-α, and NF-κB, three indicators of inflammation, were substantially higher in group 2 than in other groups, remarkably higher in groups 3 and 4 than in groups 1 and 5, and notably higher in group 5 than in group 1, but it did not differ between groups 3 and 4 (**Figure 6A-C**). Con-

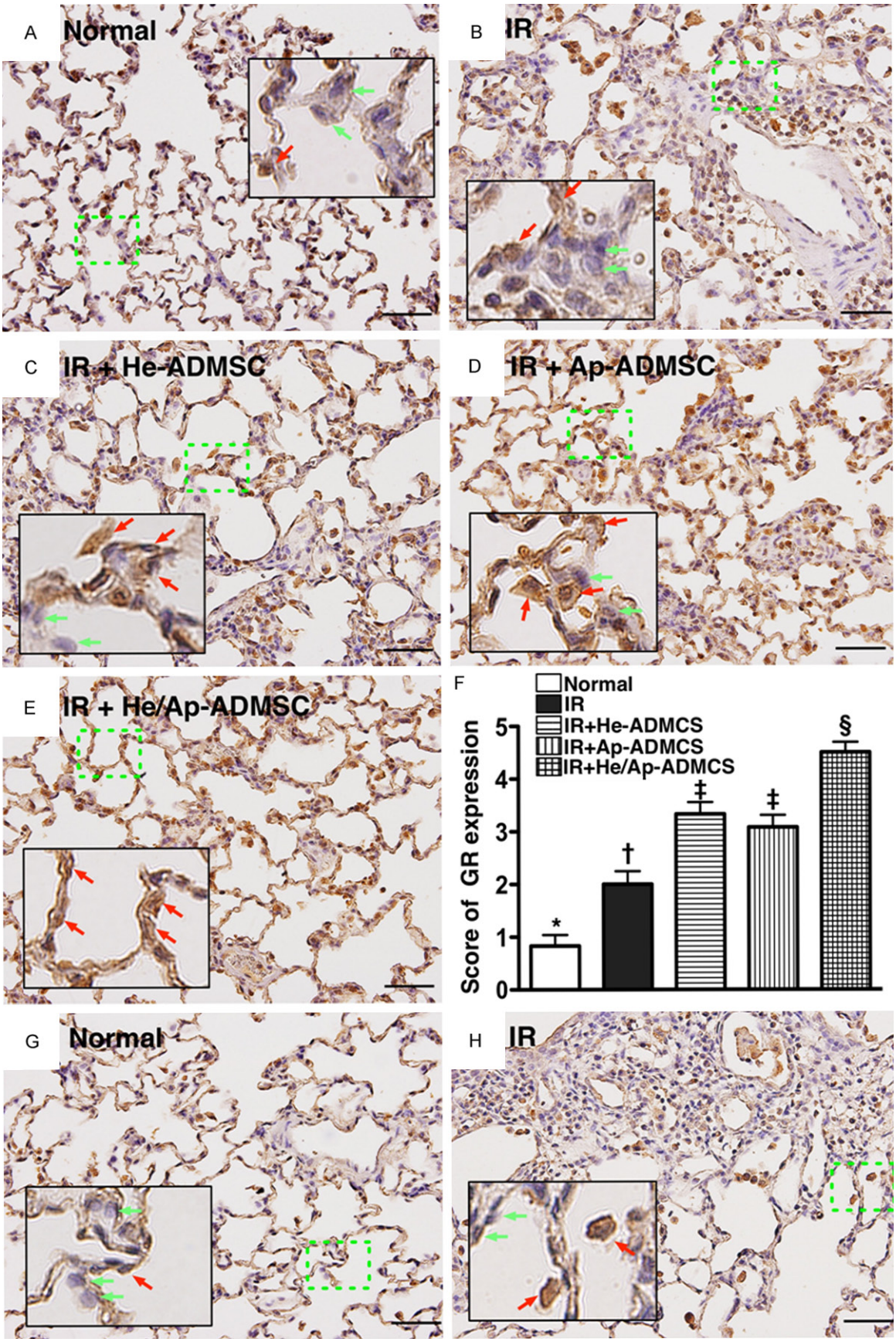
A
Normal
B
IR
C
IR + He-ADMSC
D
IR + Ap-ADMSC
E
IR + He/Ap-ADMSC
F
Normal
IR
IR+He-ADMCS
IR+Ap-ADMCS
IR+He/Ap-ADMCS
Score of GR expression
0
1
2
3
4
5
*
†
‡
‡
§
G
Normal
H
IR

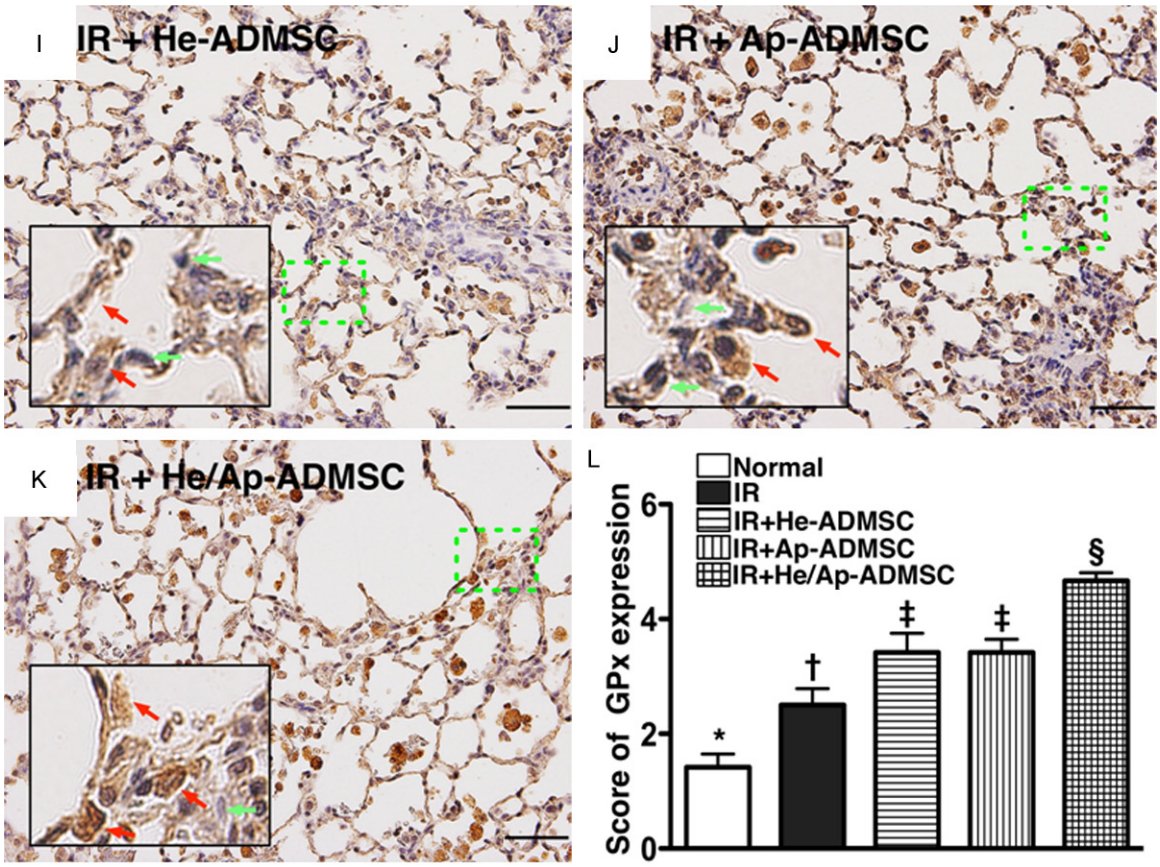

Figure 8. Immunohistochemical (IF) staining for left lung expressions of anti-oxidative markers at 72 h after ischemia-reperfusion. A-E. IF staining of glutathione reductase (GR)+ cells (brown) (200x) in lung parenchyma of the five animal groups. F. Comparison of GR expression score among the five groups. *vs. other bars with different symbols, $p < 0.0001$. G-K. IF staining of glutathione peroxidase (GPx)+ cells (brown) (200x) in lung parenchyma of the five groups. L. Comparison of GPx expression score among the five groups. *vs. other bar with different symbols, $p < 0.0001$. Scale bars at right lower corners represent 50 μm. Symbols (*, †, ‡, §) indicating significance (at 0.05 level). IR = ischemia reperfusion; He-ADMSC = healthy ADMSC (i.e. cultivated in normal medium); Sd-ADMSC = serum-deprived ADMSC. (n = 6 in each group).

versely, the mRNA expressions of HO-1, NQO 1, GR, and GPx, four anti-oxidative indicators, showed an opposite pattern compared to that of inflammatory gene expressions among the five groups (**Figure 6D-G**). More interesting finding is that the mRNA expression of IL-10, one index of anti-inflammation/immunomodulation, was significantly lower in groups 1 and 2 than in groups 3 to 5, significantly lower in group 3 than in groups 4 and 5, and notably lower in group 4 than in group 5 (**Figure 6H**). Furthermore, mRNA expression of eNOS, an indicator of endothelial integrity, showed similar pattern compared to that of anti-oxidant expression, whereas ET-1 mRNA expression, an indicator of endothelial dysfunction, exhibited a reversed pattern compared to that of eNOS among the five groups (**Figure 6I**, **6J**).

The expressions of endothelial cell markers, CD31 and vWF, and Anti-Oxidant indices, GR and GPx, in lung parenchyma

Fluorescent microscopy demonstrated significantly lower number of CD31 + (**Figure 7A-F**) and vWF + cells (**Figure 7G-L**), two indicators of endothelial cellular phenotypes, in lung parenchyma of groups 1 and 2. The number was higher in group 1 than in group 2, and notably higher in group 5 than in groups 3 and 4, but it showed no difference between groups 3 and 4.

IF staining demonstrated that the number of cells positive for GR (**Figure 8A-F**) and GPx (**Figure 8G-L**), two indicators of anti-oxidants, were highest in group 5, significantly higher in groups 3 and 4 than in groups 1 and 2, and

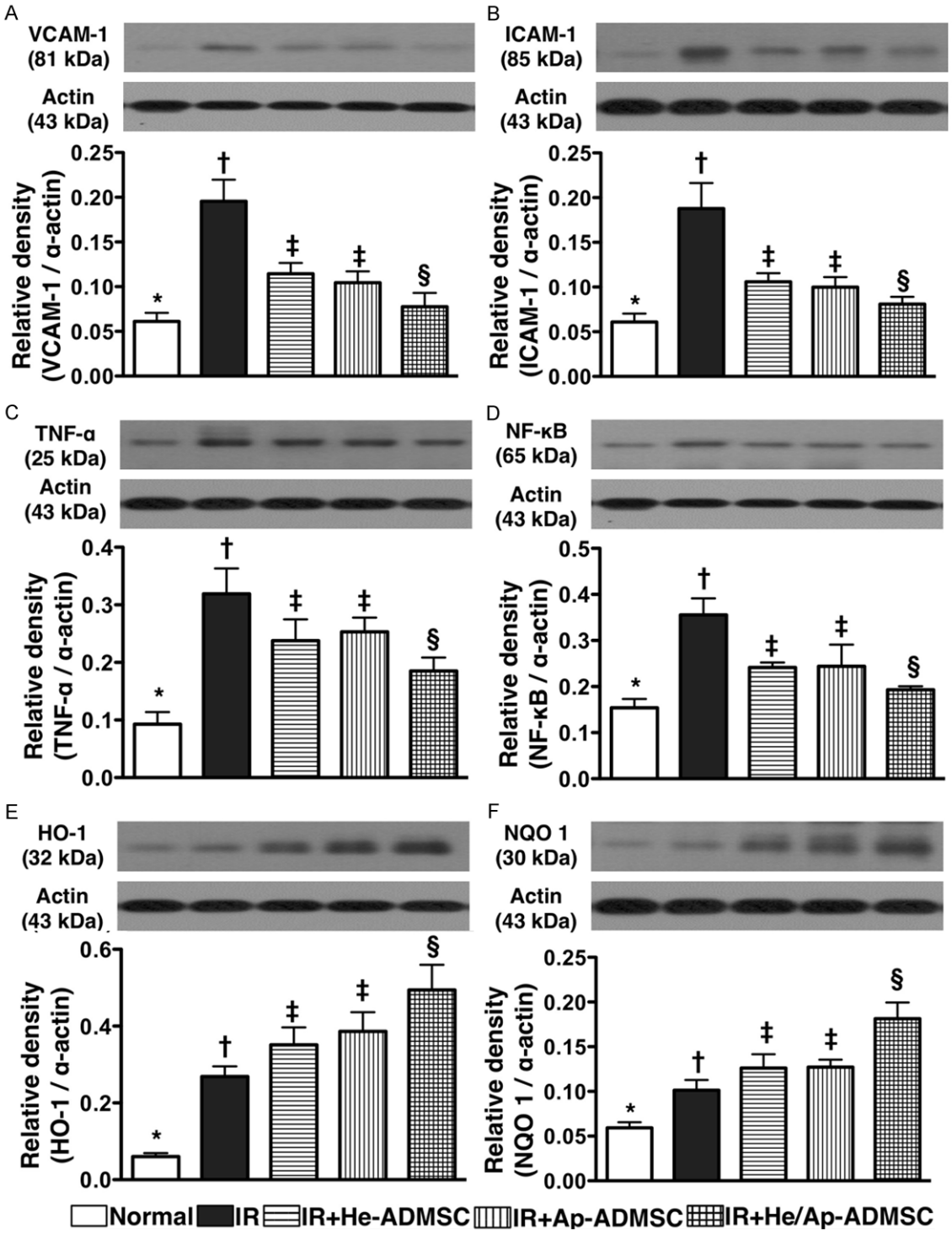

Figure 9. Changes in protein expressions of inflammatory and anti-oxidant markers in left lung parenchyma at 72 h after ischemia-reperfusion. A-D. Protein expressions of vascular cell adhesion molecule (VCAM)-1, intercellular adhesion molecule (ICAM)-1, tumor necrotic factor (TNF)-α and nuclear factor (NF)-κB in left lung. *vs. other bars with different symbols, $p < 0.001$. E and F. Protein expressions of heme oxygense (HO)-1 and NAD(P)H quinone oxidoreductase (NQO) 1. *vs. other bars with different symbols, $p < 0.001$. Symbols (*, †, ‡, §, ¶) indicating significance (at 0.05 level). IR = ischemia reperfusion; He-ADMSC = healthy ADMSC (i.e. cultivated in normal medium); Sd-ADMSC = serum-deprived ADMSC. (n = 6 in each group).

significantly higher in group 2 than in group 1, but it showed no difference between groups 3 and 4. These findings suggest that ALIRI induced an intrinsic anti-oxidant elevation for pro-

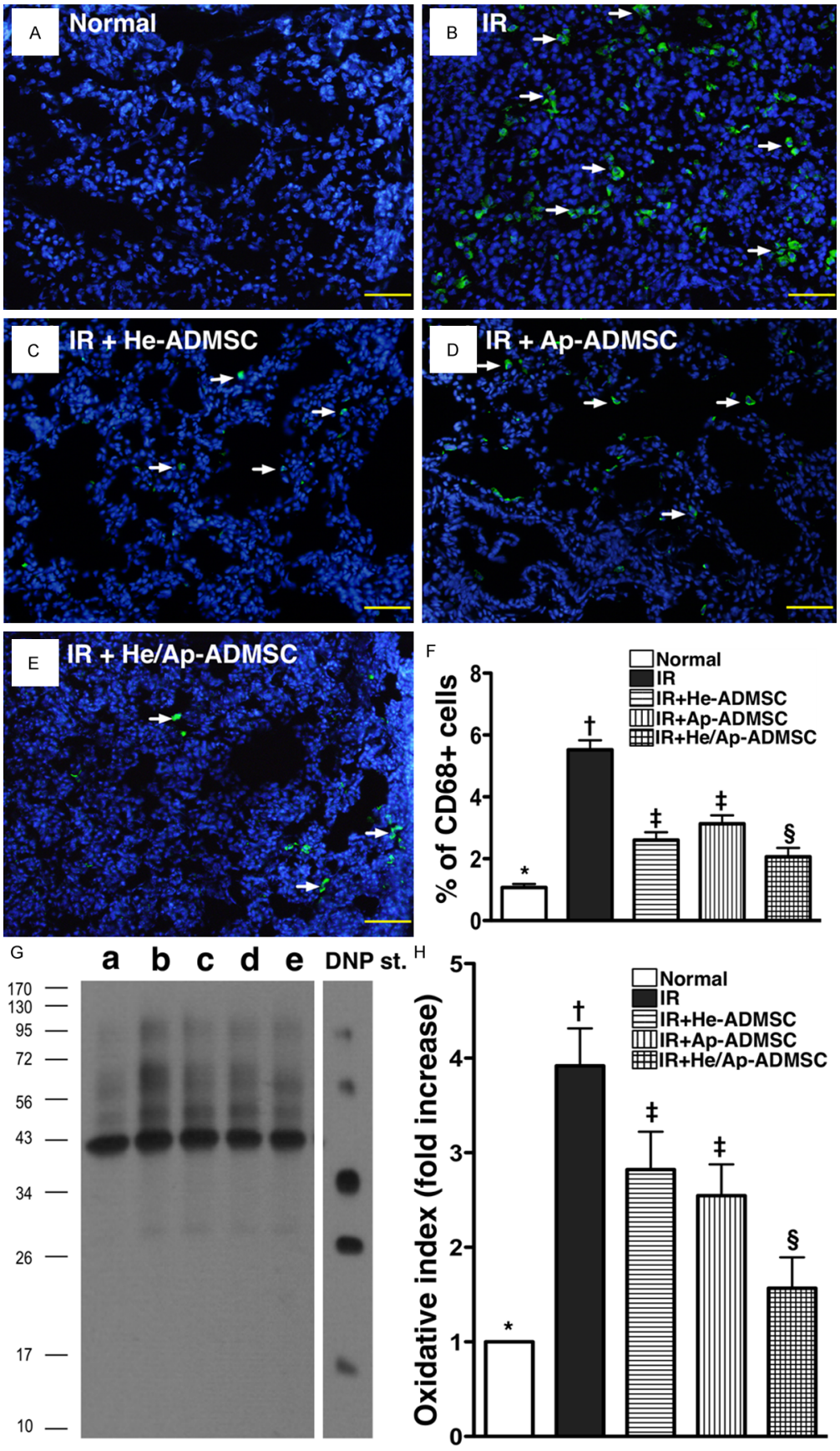
A
Normal
B
IR
C
IR + He-ADMSC
D
IR + Ap-ADMSC
E
IR + He/Ap-ADMSC
F
% of CD68+ cells
Normal
IR
IR+He-ADMSC
IR+Ap-ADMSC
IR+He/Ap-ADMSC
G
a b c d e
DNP st.
170
130
95
72
56
43
34
26
17
10
H
Oxidative index (fold increase)

Figure 10. Immunofluorescent staining for CD 68+ cells and Western blotting for oxidized protein expression in left lung parenchyma at 72 h after ischemia-reperfusion (IR). A-E. IF staining showing infiltration of left lung parenchyma with CD68+ cells (white arrows). F. Prevalence of CD68+ cells in left lung among the five animal groups at post-IR 72 h. *vs. other bars with different symbols, $p < 0.001$. G. Expression of protein carbonyls (i.e., oxidized protein), an oxidative index, in the five groups of animals (Note: Right lane and left lane shown on upper panel representing control oxidized molecular protein standard and protein molecular weight marker, respectively). DNP = 1-3 dinitrophenylhydrazone. H. Oxidative index in left lung tissue among five groups at post-IR 72 h. *vs. other bars with different symbols, $p < 0.0001$. Symbols (*, †, ‡, §) indicating significance (at 0.05 level). He-ADMSC = healthy ADMSC (i.e. cultivated in normal medium); Sd-ADMSC = serum-deprived ADMSC. (n = 6 in each group).

tection against IR in ischemic region and that ADMSC treatment further enhanced the protection.

Autologous ADMSC transfusion attenuated protein expressions of inflammatory markers and reactive oxygen species in lung parenchyma after IR injury

The protein expressions of VCAM-1, ICAM-1, TNF-α, and NF-κB, four inflammatory biomarkers, were significantly higher in group 2 than in other groups, significantly higher in groups 3 and 4 than those in groups 1 and 5, notably higher in group 5 compared with those in group 1, but it showed no difference between groups 3 and 4 following ALIRI (**Figure 9A-D**). By contrast, the protein expressions of HO-1 and NQO 1 (**Figure 9E**, **9F**), two anti-oxidative indexes, were significantly higher in groups 5 than in other groups, significantly higher in groups 3 and 4 than in groups 1 and 2 and significantly higher in group 2 than in group 1, but no difference was noted between groups 3 and 4.

Autologous ADMSC transfusion ameliorated inflammatory cell infiltration and oxidized protein expression in lung parenchyma after IR injury

IF staining demonstrated that the number of CD68 + cells, a macrophage surface marker in left lung parenchyma, was significantly higher in group 2 than in other groups, significantly higher in groups 3 and 4 than in groups 1 and 5, and significantly higher in group 5 than in group 1, but it was similar between groups 3 and 4 (**Figure 10A-F**). Similarly, the expression of oxidized protein, an indicator of oxidative stress, exhibited an identical pattern compared to that of CD68 + cells among the five groups (**Figure 10G**, **10H**).

Autologous ADMSC transfusion reduced apoptotic protein expressions in lung parenchyma after IR injury

Western blot analyses demonstrated that the protein expressions of Bax (**Figure 11A**), and the cleaved forms of caspase 3 (**Figure 11B**) and PARP (**Figure 11C**) (i.e. the active forms), three apoptotic indicators, were remarkably higher in group 2 than in other groups, notably higher in groups 3 and 4 than in groups 1 and 5, and significantly higher in group 5 than in group 1, but no difference was noted between groups 3 and 4. By contrast, the protein expression of Bcl-2, an indicator of anti-apoptosis, exhibited a reversed manner compared to that of apoptotic protein expressions among the five groups (**Figure 11D**).

Discussion

One distinctive finding in the present study is that, as compared with lung IR alone, He-ADMSC or Sd-ADMSC treatment remarkably reduced IR-induced elevation of RVSBP, an indirect evidence of pulmonary arterial hypertension (PAH). In addition, either therapeutic regimen markedly improved IR-induced hypoxemia. The most important finding in the current study is that combined therapy with He-ADMSCs and Sd-ADMSCs was superior to either alone in reversing IR-induced hypoxemia and PAH, two principal indicators of ALIRI. The results from our studies and those from others [25, 30, 32] have recently demonstrated that He-ADMSCs and bone marrow-derived mesenchymal stem cells were effective in attenuating IR-induced lung injury. Therefore, our results, in addition to supporting those of previous studies [25, 30, 32], further demonstrated that treatment with Sd-ADMSCs and mixed ADMSCs significantly contributed to even more promising functional outcomes (i.e., hypoxemia, PAH) after ALIRI. Of importance is that the findings of the present study highlight the therapeutic potential of Sd-ADMSCs in the clinical setting of acute lung injury.

It has been well documented that acute tissue/organ injuries from various etiologies frequently lead to inflammatory responses, activation of the complement cascade, and generation of ROS [8-14, 20, 30, 33]. Without prompt and effective interventional strategy, these reac-

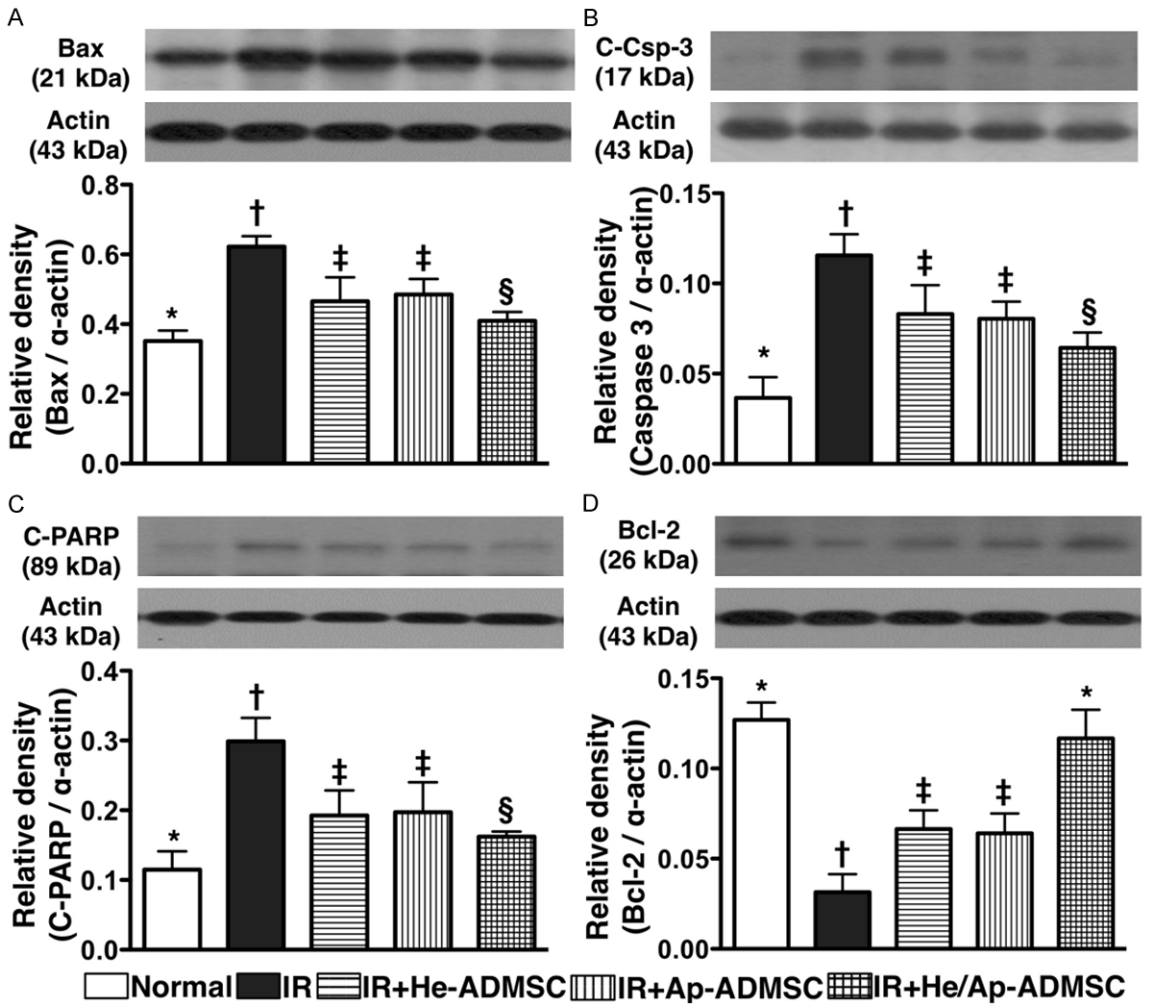

Figure 11. Changes in protein expressions of apoptotic and anti-apoptotic markers in left lung parenchyma at 72 h after Ischemia-reperfusion. A. Mitochondrial Bax expression. *vs. other bars with different symbols, $p < 0.001$. B & C. Expressions of cleaved (C-) caspase (Csp)-3 and poly(ADP-ribose) polymerase (PARP). *vs. other bars with different symbols, $p < 0.001$. D. Bcl-2 expression. *vs. other bars with different symbols, $p < 0.001$. Symbols (*, †, ‡, §) indicating significance (at 0.05 level). IR = ischemia reperfusion; He-ADMSC = healthy ADMSC (i.e. cultivated in normal medium); Sd-ADMSC = serum-deprived ADMSC. (n = 6 in each group).

tions will rapidly become progressive and further damage the tissue/organs involved [30, 33]. Consistently, the current study demonstrated that the inflammatory reactions (i.e., at gene, protein, and cellular levels) and the generation of ROS (at protein level) were markedly enhanced in animals after ALIRI. Importantly, this study showed that administration of either He-ADMSCs or Sd-ADMSCs significantly reduced IR-induced inflammatory responses and oxidative stress in an animal model. Of particular importance is that combined treatment with well-nourished and undernourished ADMSCs could provide an additional benefit in attenuating these adverse reactions. In addition to supporting the finding of our previous study that demonstrated an up-regulation of anti-oxidative activities after He-ADMSC administration [30], the results of the present study also showed that the expressions of anti-oxidant biomarkers (i.e., HO-1, NQO 1, GR, GPx) were notably enhanced after either He-ADMSC or Sd-ADMSC treatment and were further augmented following simultaneous infusion of the two cellular elements. Taken together, the alleviation of IR-elicited inflammation and oxidative stress as well as the reinforcement of anti-oxidative activities could probably explain the anatomical and histopathological improvement (**Figures 4**, **5**) and the reduction of apoptosis (**Figure 11**) in the lungs after either He-ADMSCs or Sd-ADMSCs administration and particularly

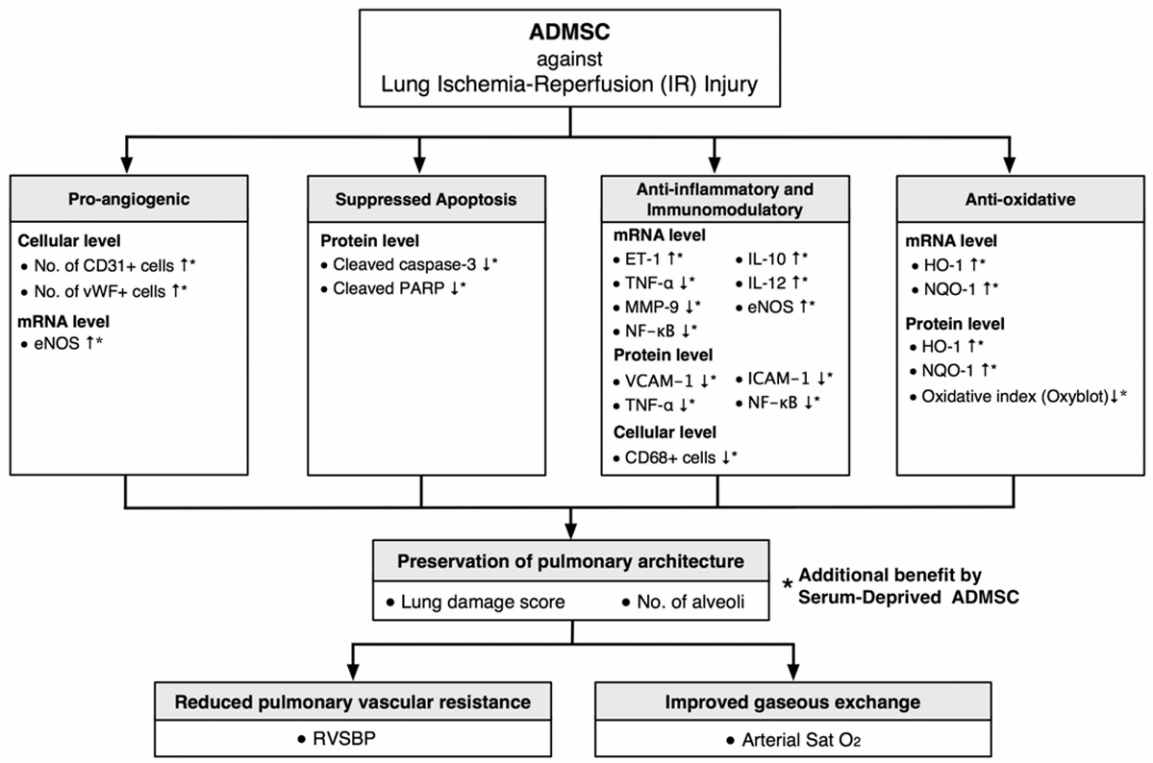

Figure 12. Proposed mechanisms underlying the effects of apoptotic and non-apoptotic adipose-derived mesenchymal stem cell treatment on acute lung IR injury in a rat model based on findings of the present study. ADMSC = adipose-derived mesenchymal stem cell; vWF = von Willebrand factor; eNOS = endothelial nitric oxide synthase; PARP = poly(ADP-ribose) polymerase; ET = endothelin; TNF = tumor necrosis factor; MMP = matrix metalloproteinase; NF = nuclear factor; IL = interleukin; VCAM = vascular cell adhesion molecule; ICAM = intercellular adhesion molecule; HO = heme oxygenase; NQO = NAD(P)H dehydrogenase (quinone); RVSBP = right ventricular systolic blood pressure.

following combined cellular treatment in animals after ALIRI.

Although healthy and apoptotic mesenchymal stem cells have been proposed to possess immune-modulating property [28, 29], the precise mechanism remains unclear. Interestingly, in the current study, the mRNA expression of IL-10, an index of anti-inflammation/immunomodulation, was significantly elevated in the left lungs of animals following Sd-ADMSC treatment compared with those receiving He-ADMSCs. The expression was further enhanced in animals after treatment with combined He-ADMSCs and Sd-ADMSCs.

Another intriguing finding of the in vitro study is that ELISA demonstrated markedly increased levels of TGF-β, IL-4, and IL-10, three indicators of anti-inflammation/immunomodulation, in conditioned medium derived from He-ADMSCs compared to that derived from Sd-ADMSCs. On the other hand, the level of PGE-2, also an indicator of anti-inflammation/immunomodulation, in the cultured medium displayed an opposite pattern (**Figure 2E**). Moreover, the level of PGE-2 was notably increased in conditioned medium from culturing macrophages with He-ADMSC-derived medium compared to that from culturing macrophages with Sd-ADMSC-derived medium (**Figure 2Fa-Fc**). On the other hand, the levels of IL-4 and PGE-2 were notably increased in the medium from co-culturing macrophages with Sd-ADMSCs compared to from co-culturing macrophages with He-ADMSCs (**Figure 2Fd-Ff**). Our findings, in addition to supporting the "dying stem cell hypothesis" that proposes the beneficial immunomodulatory roles of apoptotic stem cells [29], highlight that the anti-inflammatory and immunomodulatory properties of He-ADMSCs may be through the effect of ant-inflammatory cytokines, whereas Sd-ADMSCs may exert these actions via the regulation of innate and adaptive immunity through cell to cell interaction (i.e., macrophages and Sd-ADMSCs).

Our recent study has shown that treatment of acute lung IR injury in rats with He-ADMSCs enhanced cellular expression of CD31 and vWF, two endothelial cell indicators, in lung parenchyma [30]. Another intriguing finding in the current study is that the transfusion of Sd-ADMSCs further reinforced pulmonary expression of these two endothelial cell surface markers. These findings not only extend those of our previous study [30], but could also explain the enhanced mRNA expression of eNOS and suppressed mRNA expression of ET-1 in the lungs after IR following infusion of either type of cellular element and the assorted ADMSCs. In this way, the findings of the current study strengthen those of our recent reports [28, 29].

Study limitations

It is well known that the initiation and propagation of immune reaction in mammals is complicated with interactions among the humoral, cellular, and complement systems. The results of the present study, therefore, may not reflect the full picture of in vivo ADMSC-mediated immunomodulation in the setting of IR-induced lung injury. The proposed mechanisms underlying the observations of attenuated inflammation and improved pulmonary histology after IR injury of the lungs based on our findings have been summarized in **Figure 12**.

Conclusion

Combined therapy with assorted ADMSCs markedly attenuated ALIRI probably through suppressing acute immune response, inflammatory reaction, oxidative stress, and ROS generation.

Acknowledgements

This study was supported by a program grant from Chang Gung Memorial Hospital, Chang Gung University (Grant number: CMRPG8A0-791).

Disclosure of conflict of interest

None.

Address correspondence to: Hsueh-Wen Chang, Department of Biological Sciences, National Sun Yat-Sen University, Kaohsiung, Taiwan. E-mail: hwchang@mail.nsysu.edu.tw; Hon-Kan Yip, Institute of Shock Wave Medicine and Tissue Engineering, Kaohsiung Chang Gung Memorial Hospital and Chang Gung University College of Medicine, Kaohsiung, Taiwan. E-mail: han.gung@msa.hinet.net

References

[1] Rubenfeld GD and Herridge MS. Epidemiology and outcomes of acute lung injury. Chest 2007; 131: 554-562.

[2] Fan E, Wilcox ME, Brower RG, Stewart TE, Mehta S, Lapinsky SE, Meade MO and Ferguson ND. Recruitment maneuvers for acute lung injury: a systematic review. Am J Respir Crit Care Med 2008; 178: 1156-1163.

[3] Esteban A, Anzueto A, Frutos F, Alia I, Brochard L, Stewart TE, Benito S, Epstein SK, Apezteguia C, Nightingale P, Arroliga AC, Tobin MJ; Mechanical Ventilation International Study G. Characteristics and outcomes in adult patients receiving mechanical ventilation: a 28-day international study. JAMA 2002; 287: 345-355.

[4] Bittner HB, Binner C, Dahlberg P and Mohr FW. Reducing ischemia-reperfusion injury in clinical lung transplantation. Transplant Proc 2007; 39: 489-492.

[5] Chamogeorgakis TP, Kostopanagiotou GG, Kalimeris CA, Kabouroglou GI, Kourtesis AN, Routsi CI, Dima CC and Toumpoulis IK. Effect of N-acetyl-L-cysteine on lung ischaemia reperfusion injury in a porcine experimental model. ANZ J Surg 2008; 78: 72-77.

[6] Chang H, Huang KL, Li MH, Hsu CW, Tsai SH and Chu SJ. Manipulations of core temperatures in ischemia-reperfusion lung injury in rabbits. Pulm Pharmacol Ther 2008; 21: 285-291.

[7] Botha P, Jeyakanthan M, Rao JN, Fisher AJ, Prabhu M, Dark JH and Clark SC. Inhaled nitric oxide for modulation of ischemia-reperfusion injury in lung transplantation. J Heart Lung Transplant 2007; 26: 1199-1205.

[8] Peek GJ, Mugford M, Tiruvoipati R, Wilson A, Allen E, Thalanany MM, Hibbert CL, Truesdale A, Clemens F, Cooper N, Firmin RK, Elbourne D and collaboration CT. Efficacy and economic assessment of conventional ventilatory support versus extracorporeal membrane oxygenation for severe adult respiratory failure (CESAR): a multicentre randomised controlled trial. Lancet 2009; 374: 1351-1363.

[9] Wolf PS, Merry HE, Farivar AS, McCourtie AS and Mulligan MS. Stress-activated protein kinase inhibition to ameliorate lung ischemia reperfusion injury. J Thorac Cardiovasc Surg 2008; 135: 656-665.

[10] McCourtie AS, Farivar AS, Woolley SM, Merry HE, Wolf PS, Mackinnon-Patterson B, Keech JC, Fitzsullivan E and Mulligan MS. Alveolar

macrophage secretory products effect type 2 pneumocytes undergoing hypoxia-reoxygenation. Ann Thorac Surg 2008; 86: 1774-1779.

[11] Hashimoto N, Takeyoshi I, Tsutsumi H, Sunose Y, Tokumine M, Totsuka O, Ohwada S, Matsumoto K and Morishita Y. Effects of a bradykinin B(2) receptor antagonist on ischemia-reperfusion injury in a canine lung transplantation model. J Heart Lung Transplant 2004; 23: 606-13.

[12] Seekamp A, Mulligan MS, Till GO, Smith CW, Miyasaka M, Tamatani T, Todd RF 3rd and Ward PA. Role of beta 2 integrins and ICAM-1 in lung injury following ischemia-reperfusion of rat hind limbs. Am J Pathol 1993; 143: 464-472.

[13] Iwata T, Chiyo M, Yoshida S, Smith GN Jr, Mickler EA, Presson R Jr, Fisher AJ, Brand DD, Cummings OW and Wilkes DS. Lung transplant ischemia reperfusion injury: metalloprotease inhibition down-regulates exposure of type V collagen, growth-related oncogene-induced neutrophil chemotaxis, and tumor necrosis factor-alpha expression. Transplantation 2008; 85: 417-426.

[14] Garcia-Covarrubias L, Manning EW 3rd, Sorell LT, Pham SM and Majetschak M. Ubiquitin enhances the Th2 cytokine response and attenuates ischemia-reperfusion injury in the lung. Crit Care Med 2008; 36: 979-982.

[15] Geudens N, Wuyts WA, Rega FR, Vanaudenaerde BM, Neyrinck AP, Verleden GM, Lerut TE and Van Raemdonck DE. N-acetyl cysteine attenuates the inflammatory response in warm ischemic pig lungs. J Surg Res 2008; 146: 177-183.

[16] Kostopanagiotou GG, Kalimeris KA, Arkadopoulos NP, Pafiti A, Panagopoulos D, Smyrniotis V, Vlahakos D, Routsi C, Lekka ME and Nakos G. Desferrioxamine attenuates minor lung injury following surgical acute liver failure. Eur Respir J 2009; 33: 1429-36.

[17] Zheng S, Zhang WY, Zhu LW, Lin K and Sun B. Surfactant and inhaled nitric oxide in rats alleviate acute lung injury induced by intestinal ischemia and reperfusion. J Pediatr Surg 2001; 36: 980-984.

[18] Veldhuizen RA, Marcou J, Yao LJ, McCaig L, Ito Y and Lewis JF. Alveolar surfactant aggregate conversion in ventilated normal and injured rabbits. Am J Physiol 1996; 270: L152-158.

[19] Davani S, Marandin A, Mersin N, Royer B, Kantelip B, Herve P, Etievent JP and Kantelip JP. Mesenchymal progenitor cells differentiate into an endothelial phenotype, enhance vascular density, and improve heart function in a rat cellular cardiomyoplasty model. Circulation 2003; 108: II253-258.

[20] Yuen CM, Sun CK, Lin YC, Chang LT, Kao YH, Yen CH, Chen YL, Tsai TH, Chua S, Shao PL, Leu S and Yip HK. Combination of cyclosporine and erythropoietin improves brain infarct size and neurological function in rats after ischemic stroke. J Transl Med 2011; 9: 141.

[21] Schachinger V, Assmus B, Erbs S, Elsasser A, Haberbosch W, Hambrecht R, Yu J, Corti R, Mathey DG, Hamm CW, Tonn T, Dimmeler S and Zeiher AM. Intracoronary infusion of bone marrow-derived mononuclear cells abrogates adverse left ventricular remodelling post-acute myocardial infarction: insights from the reinfusion of enriched progenitor cells and infarct remodelling in acute myocardial infarction (REPAIR-AMI) trial. Eur J Heart Fail 2009; 11: 973-979.

[22] Kolvenbach R, Kreissig C, Ludwig E and Cagiannos C. Stem cell use in critical limb ischemia. J Cardiovasc Surg (Torino) 2007; 48: 39-44.

[23] Assmus B, Rolf A, Erbs S, Elsasser A, Haberbosch W, Hambrecht R, Tillmanns H, Yu J, Corti R, Mathey DG, Hamm CW, Suselbeck T, Tonn T, Dimmeler S, Dill T, Zeiher AM, Schachinger V and Investigators RA. Clinical outcome 2 years after intracoronary administration of bone marrow-derived progenitor cells in acute myocardial infarction. Circ Heart Fail 2010; 3: 89-96.

[24] Tendera M, Wojakowski W, Ruzyllo W, Chojnowska L, Kepka C, Tracz W, Musialek P, Piwowarska W, Nessler J, Buszman P, Grajek S, Breborowicz P, Majka M and Ratajczak MZ. Intracoronary infusion of bone marrow-derived selected CD34 + CXCR4 + cells and non-selected mononuclear cells in patients with acute STEMI and reduced left ventricular ejection fraction: results of randomized, multicentre Myocardial Regeneration by Intracoronary Infusion of Selected Population of Stem Cells in Acute Myocardial Infarction (REGENT) Trial. Eur Heart J 2009; 30: 1313-1321.

[25] Salgar S, Manning E, Ruiz P and Pham S. Mesenchymal Stem Cell (MSC) Therapy To Prevent Ischemia-Reperfusion Injury in Lung Transplantation. J Immunol 2010; 184: 145.124.

[26] Tomita S, Li RK, Weisel RD, Mickle DA, Kim EJ, Sakai T and Jia ZQ. Autologous transplantation of bone marrow cells improves damaged heart function. Circulation 1999; 100: II247-256.

[27] Mangi AA, Noiseux N, Kong D, He H, Rezvani M, Ingwall JS and Dzau VJ. Mesenchymal stem cells modified with Akt prevent remodeling and restore performance of infarcted hearts. Nat Med 2003; 9: 1195-1201.

[28] Le Blanc K, Tammik L, Sundberg B, Haynesworth SE and Ringden O. Mesenchymal stem

cells inhibit and stimulate mixed lymphocyte cultures and mitogenic responses independently of the major histocompatibility complex. Scand J Immunol 2003; 57: 11-20.

[29] Thum T, Bauersachs J, Poole-Wilson PA, Volk HD and Anker SD. The dying stem cell hypothesis: immune modulation as a novel mechanism for progenitor cell therapy in cardiac muscle. J Am Coll Cardiol 2005; 46: 1799-1802.

[30] Sheu JJ, Chua S, Sun CK, Chang LT, Yen CH, Wu CJ, Fu M and Yip HK. Intra-coronary administration of cyclosporine limits infarct size, attenuates remodeling and preserves left ventricular function in porcine acute anterior infarction. Int J Cardiol 2011; 147: 79-87.

[31] Zhu W, Chen J, Cong X, Hu S and Chen X. Hypoxia and serum deprivation-induced apoptosis in mesenchymal stem cells. Stem Cells 2006; 24: 416-425.

[32] Gupta N, Su X, Popov B, Lee JW, Serikov V and Matthay MA. Intrapulmonary delivery of bone marrow-derived mesenchymal stem cells improves survival and attenuates endotoxin-induced acute lung injury in mice. J Immunol 2007; 179: 1855-1863.

[33] Frangogiannis NG. The immune system and cardiac repair. Pharmacol Res 2008; 58: 88-111.